Earth's Future

RESEARCH ARTICLE
10.1029/2022EF003104

The Future of Soils in the Midwestern United States

J. S. Kwang[1,2], E. A. Thaler[1,3], and I. J. Larsen[1]

[1]Department of Earth, Geographic, and Climate Sciences, University of Massachusetts, Amherst, MA, USA, [2]Now at Saint Anthony Falls Laboratory, University of Minnesota, Minneapolis, MN, USA, [3]Now at Earth and Environmental Sciences Division, Los Alamos National Laboratory, Los Alamos, NM, USA

Key Points:

- Soil and soil carbon redistribution are predicted across the Midwestern United States over centennial timescales using a landscape evolution model
- In the next century, we predict soil and soil organic carbon (SOC) erosion to be 8.8 (+1.9/−2.1) and 0.17 (+0.03/−0.04) Pg, respectively
- We predict that the total adoption of low-intensity tillage practices can reduce soil and SOC erosion by 95% after 100 years

Supporting Information:

Supporting Information may be found in the online version of this article.

Correspondence to:

J. S. Kwang,
kwang004@umn.edu

Citation:

Kwang, J. S., Thaler, E. A., & Larsen, I. J. (2023). The future of soils in the Midwestern United States. *Earth's Future*, *11*, e2022EF003104. https://doi.org/10.1029/2022EF003104

Received 11 AUG 2022
Accepted 14 APR 2023

Author Contributions:

Conceptualization: J. S. Kwang, E. A. Thaler, I. J. Larsen
Data curation: J. S. Kwang, E. A. Thaler
Formal analysis: J. S. Kwang
Funding acquisition: I. J. Larsen
Investigation: J. S. Kwang, E. A. Thaler
Methodology: J. S. Kwang, E. A. Thaler, I. J. Larsen
Resources: I. J. Larsen
Software: J. S. Kwang
Supervision: I. J. Larsen
Validation: J. S. Kwang
Visualization: J. S. Kwang
Writing – original draft: J. S. Kwang

Abstract Soil is the source of the vast majority of food consumed on Earth, and soils constitute the largest terrestrial carbon pool. Soil erosion associated with agriculture reduces crop productivity, and the redistribution of soil organic carbon (SOC) by erosion has potential to influence the global carbon cycle. Tillage strongly influences the erosion and redistribution of soil and SOC. However, tillage is rarely considered in predictions of soil erosion in the U.S.; hence regionwide estimates of both the current magnitude and future trends of soil redistribution by tillage are unknown. Here we use a landscape evolution model to forecast soil and SOC redistribution in the Midwestern United States over centennial timescales. We predict that present-day rates of soil and SOC erosion are 1.1 ± 0.4 kg $\cdot$ m^{-2} $\cdot$ yr^{-1} and 12 ± 4 g $\cdot$ m^{-2} $\cdot$ yr^{-1}, respectively, but these rates will rapidly decelerate due to diffusive evolution of topography and the progressive depletion of SOC in eroding soil profiles. After 100 years, we forecast that 8.8 (+1.9/−2.1) Pg of soil and 0.17 (+0.03/−0.04) Pg of SOC will have eroded, causing the surface concentration of SOC to decrease by 4.4% (+0.9/−1.1%). Model simulations that include more widespread adoption of low-intensity tillage (i.e., no-till farming) determine that soil redistribution, SOC redistribution, and surficial SOC loss after 100 years would decrease by ∼95% if low-intensity tillage is fully adopted. Our findings indicate that low-intensity tillage could greatly decrease soil degradation and that the potential for agricultural soil erosion to influence the global carbon cycle will diminish with time due to a reduction in SOC burial.

Plain Language Summary Plow-based agriculture has accelerated soil erosion rates by one to two orders of magnitude, which diminishes crop productivity and has the potential to impact the carbon cycle. Using a numerical model, we calculate that present-day rate of soil and soil organic carbon (SOC) erosion are 1.1 ± 0.4 kg $\cdot$ m^{-2} $\cdot$ yr^{-1} and 12 ± 4 g $\cdot$ m^{-2} $\cdot$ yr^{-1}, respectively and predict that 8.8 (+1.9/−2.1) Pg of soil and 0.17 (+0.03/−0.04) Pg of SOC will be eroded in the Midwestern United States over the next century. Compared to other measured rates of soil and SOC erosion, the predicted rates are relatively high and have the potential to degrade soil and influence the carbon cycle. With our model, we simulated the more widespread adoption of low-intensity tillage (i.e., no-till farming) and found that the full adoption of low-intensity tillage would reduce soil and SOC erosion by ∼95% over the next 100 years. Therefore, our results indicate that further adoption of low-intensity tillage has the potential to greatly reduce soil and SOC erosion and contribute to soil sustainability.

1. Introduction

Healthy soils provide essential ecosystem services and supply most of the food for human livelihood (Kopittke et al., 2019; Shukla et al., 2019). Rates of human-induced, agricultural soil erosion are estimated to outpace natural soil production rates by one to two orders of magnitude (Evans et al., 2019; Montgomery, 2007b; Quarrier et al., 2022; Reusser et al., 2015; Shukla et al., 2019). The imbalance between rates of production and erosion means that the quality of soil in agricultural fields has declined (Montgomery, 2007b; Thaler et al., 2021). Degraded soil quality can lead to geopolitical conflict, food insecurity, and increased dependence on synthetic fertilizers that impair aquatic ecosystems and human health (Amundson et al., 2015; Borrelli et al., 2017; Weyer et al., 2001). Therefore, decision making that ensures human security (Amundson et al., 2015) requires careful consideration of the future of soil.

Agricultural soil erosion first removes the uppermost A-horizon soils (Lindstrom et al., 1990; Thaler et al., 2021). A-horizon soils contain the largest fraction of soil organic carbon (SOC) and are essential for nutrient and water retention and crop productivity (Fenton et al., 2005; Lal, 2006). Because soils provide 95%–98.8% of the food required by humans (FAO UN, 2015; Kopittke et al., 2019), forecasts of soil erosion and changes in SOC are

Writing – review & editing: J. S. Kwang, E. A. Thaler, I. J. Larsen

needed to predict the long-term trends in soil productivity, and such predictions are required to guide decision making regarding food security in light of the growing global population (Shukla et al., 2019).

Soil stores the largest pool of terrestrial organic carbon (Doetterl et al., 2016), and accelerated rates of soil erosion and SOC redistribution have the potential to impact the global carbon cycle (Lal, 2003; Quinton et al., 2010; Stallard, 1998). However, there is debate about the magnitude and direction of the exchange of carbon between soil and the atmosphere (Berhe et al., 2007; Billings et al., 2010, 2019; Doetterl et al., 2016; Lal, 2019; Van Oost et al., 2007; Van Oost & Six, 2023). Mineralization of displaced agricultural soils could lead to CO_2 emissions (Lal, 2003). However, if SOC transported with soil is buried before it can mineralize, and dynamic replacement of carbon occurs where soils have been eroded (Harden et al., 1999), CO_2 is sequestered (Berhe et al., 2007; Liu et al., 2003). Therefore, to assess whether agricultural soil erosion acts as a net sink or source of atmospheric CO_2, the transport and fate of SOC in the landscape must be considered (Amundson et al., 2015; Billings et al., 2019; Blair et al., 2022; Doetterl et al., 2016; Lal, 2003; Van Oost et al., 2007). Hence, understanding the potential impacts of future soil erosion on the global carbon cycle requires detailed predictions of SOC redistribution.

2. Midwestern United States (U.S.) Soils and Erosion Modeling

In this study, we focus on the agricultural landscape of the Midwestern U.S. (Figure 1). The Midwestern U.S. is one of the most agriculturally productive regions in the world (U.S. Department of Agriculture, 2020) due to the abundance of fertile, organic carbon-rich mollisol soils that developed primarily from Pleistocene glacial till and loess deposits (Natural Resources Conservation Service, 2021). During the Pleistocene, ice sheets repeatedly covered much of this region. The most recent glaciation occurred ~14.5 ka, when the Des Moines Lobe of the Laurentide Ice Sheet reached its southernmost extent (Dalton et al., 2020). The present-day distributions of SOC and tillage practices are strongly influenced by the regional glacial history, with more SOC and less low-intensity tillage in the most recently glaciated areas (Figure 1). The post-glacial climate facilitated the development of tallgrass prairie vegetation (Samson & Knopf, 1994), but the conversion from prairie to agricultural fields has

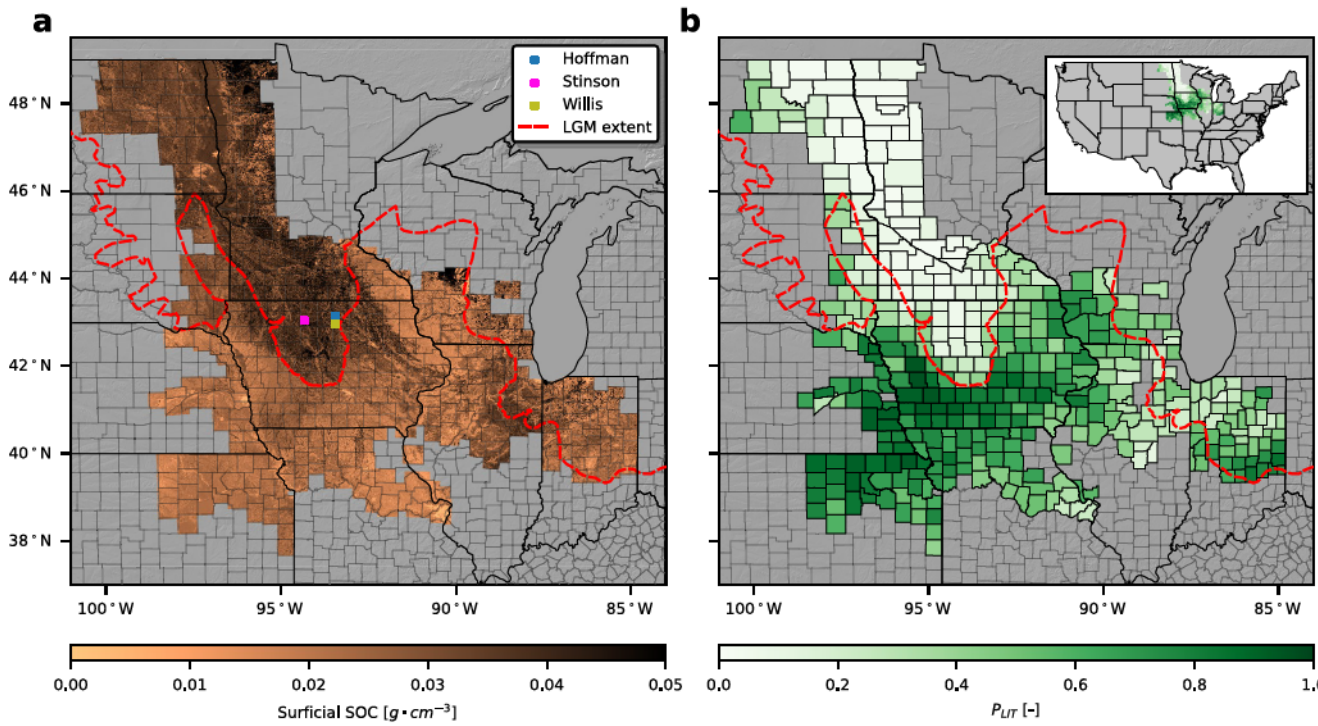

Figure 1. The study area in the Midwestern United States showing surficial soil organic carbon (SOC) concentrations (a) and the proportion of area in each county that uses low-intensity tillage, P_{LIT} (b). Surficial SOC data are the concentration from the upper 5 cm of soil from the gridded Soil Survey Geographic Database (Soil Survey Staff, 2020). The colored counties define the spatial extent of our regional modeling. P_{LIT} values are remote sensing-based data from Azzari et al. (2019). The squares in (a) show the location of three sites (Hoffman, Stinson, Willis) where we conducted field-scale modeling. The dashed red line denotes the maximum ice sheet extent during the Last Glacial Maximum (Dalton et al., 2020).

led to a drastic acceleration in erosion rates (Quarrier et al., 2022; Thaler et al., 2022) and the removal of roughly one-third of the A-horizon soils from agricultural fields (Thaler et al., 2021). Soil degradation in the region is estimated to reduce crop yield by 6%, leading to $2.8 billion in economic losses annually (Thaler et al., 2021).

Soil erosion rates in the U.S. are often predicted with empirically-based models, such as the Revised Universal Soil Loss Equation (Borrelli et al., 2017; Nadeu et al., 2015; Renard et al., 1997; U.S. Department of Agriculture, 2018) or the physically-based Water Erosion Prediction Project model (Gelder et al., 2018; Laflen et al., 1991). However, here we use the landscape evolution model—soil organic carbon (LEM-SOC) model (Kwang et al., 2022). Unlike other models, LEM-SOC allows us to track the 3-dimensional movement of soil and SOC as they are redistributed across the landscape. Our model differs from soil erosion models that estimate the export of sediment, that is, sediment yield (Arnold et al., 1998; Laflen et al., 1991; Van Oost et al., 2000); instead, LEM-SOC predicts the internal redistribution of soil and SOC. In the Midwestern U.S., the majority of soil that is eroded is transported only a short distance before it is deposited, or redistributed; less than 10% of eroded soil is estimated to be exported from watersheds (Blair et al., 2022). Hence, our modeling focusses on the redistribution of soil and SOC that occurs within agricultural fields. Predictions of large-scale SOC fluxes often assume soil erosion rates are constant in time (Lal & Pimentel, 2008; Van Oost et al., 2007), but the impact of soil erosion on the global carbon cycle requires the consideration of long-term changes in both soil erosion rates and SOC concentrations in the eroded soil (Kuhn et al., 2009). LEM-SOC simulates such long term-changes and captures the fine-scale changes in topography that strongly influence the distribution of SOC in the Midwestern U.S. (Kwang et al., 2022; Thaler et al., 2021, 2022), which are not captured by models that do not explicitly simulate landscape evolution or topographic change.

Here we forecast soil erosion and SOC redistribution over the next 500 years but focus our analysis on predictions for the next century, which are most relevant for policy making. We model the redistribution of SOC via diffusive soil transport without also simulating water erosion, because this approach well-explains spatial patterns of soil and SOC loss in agricultural fields in the Midwestern U.S. (Kwang, Thaler, Quirk, et al., 2022). Conceptually, our model predicts soil redistribution caused by tillage, which is the primary driver of diffusive soil transport in agricultural settings (Doetterl et al., 2012, 2016; Kwang, Thaler, Quirk, et al., 2022; Van Oost et al., 2005). The main inputs of the model are digital elevation models (DEMs) and a 3-dimensional SOC pedostratigraphy. The model only requires the specification of two physical parameters: a hillslope diffusion coefficient, D, and a plow layer thickness, L_p. SOC dynamics, such as dynamic replacement and mineralization, are not simulated in LEM-SOC, but LEM-SOC has been shown to accurately predict spatial patterns of SOC with transport mechanics only (Kwang, Thaler, Quirk, et al., 2022).

3. Materials and Methods

3.1. Input Data

The initial topography was generated by merging and resampling LiDAR-derived DEMs from individual state repositories to create a regionwide DEM with 4-m pixel resolution. We limited our analysis to areas that are agricultural fields and removed areas with anomalous topographic curvature values from the DEM. Agricultural croplands were selected by clipping the DEM to the Herbaceous Agriculture raster from the U.S. Geological Survey Gap Analysis Program data set (Jennings, 2000), which removed areas with non-agricultural land from the analysis. We also removed streams and rivers from the DEM using a 50-m buffer around flowlines identified by the National Hydrography Data set (U.S. Geological Survey, 2021), transit lines (e.g., roads, railways) using a 30-m buffer around transit lines from the National Transportation Data set (U.S. Geological Survey, 2020), and property boundaries (which often coincide with fence lines or rows of trees that have anomalous curvature values, even in bare-earth DEMs) delineated by the Agricultural Conservation Planning Framework data set (Tomer et al., 2017). Areas with slope gradients that exceed 3.0 (tangent of slope) or 300% (percent slope) with a 5-m buffer were also removed, as such topographic anomalies represent features such as power lines and electrical towers that were still present after the previous filters were applied. Such areas are also too steep to cultivate.

The initial 3-dimensional distribution of SOC is based on the gridded Soil Survey Geographic Database (gSSURGO) (Soil Survey Staff, 2020). The gSSURGO database contains SOC values for depth intervals of 0–5, 5–20, 20–50, 50–100, 100–150, 150+ cm at a spatial resolution of 10 m. The deepest increment extends from 150 cm to the deepest reported depth in the soil profile, which varies. We resampled the gSSURGO data

to a 4-m pixel resolution grid using bilinear interpolation, to match the spatial resolution of the DEM. Although the gSSURGO data set is based on soil surveys conducted over decades, we assume its values represent current (2020 CE) distributions of SOC. Past research found that field measurements of SOC compared adequately with SSURGO values in Louisiana, USA ($R^2 = 0.63$) (Zhong & Xu, 2011) and soils derived from glacial parent materials in New York ($R^2 = 0.53$) (Mikhailova et al., 2016). Further, SSURGO estimates of SOC have been shown to accurately capture the range of SOC values at field scales (Gelder et al., 2011) in central Iowa. We also ran field-scale simulations at three sites (see Text S1 in Supporting Information S1) to compare field estimated and gSSURGO SOC values and found correlations comparable to those from prior studies ($R^2 = 0.47$ to 0.69) (Figures S1 and S2 in Supporting Information S1).

3.2. Landscape Evolution Model—Soil Organic Carbon (LEM-SOC)

We simulate the erosion, transport, and deposition of soil and SOC using the LEM-SOC model (Kwang, Thaler, Quirk, et al., 2022). In LEM-SOC, the evolution of topography is modeled using a linear diffusion equation:

$$\frac{\partial \eta}{\partial t} = D\nabla^2\eta \tag{1}$$

where η is elevation, D is a diffusion coefficient, and t is time. In Equation 1, regions with concave-upward topography experience deposition and regions with convex-upward topography erode. Soil flux by tillage, q, is a function of slope gradient (tangent), $\nabla\eta$, and D.

$$q = -D\nabla\eta \tag{2}$$

The mass flux of SOC is the product of the flux of soil and the SOC concentration in the soil that is being transported. Within the model, the plow layer, or depth of tillage, defines the soil that is transported in each time-step. The redistribution of SOC in the plow layer is determined with the following equation:

$$L_p\frac{\partial \mathrm{SOC}_p}{\partial t} = \mathrm{SOC}_{\mathrm{int}}\nabla\cdot q - \nabla\cdot(\mathrm{SOC}_p q) \tag{3}$$

where L_p is a plow depth, SOC_p is the soil organic carbon concentration in the plow layer, and $\mathrm{SOC}_{\mathrm{int}}$ is an interface term. At each point in the landscape, the soil column is vertically partitioned into a plow layer and a subsoil layer (e.g., weathered glacial till or loess i.e., beneath the plow layer). The plow layer extends to distance, L_p, below the surface and is assumed to be well-mixed, such that the SOC concentration does not vary as a function of depth within the plow layer. We assume that soil and SOC within the subsoil layer does not undergo transport; however, the subsoil layer interacts with the plow layer. The interaction between the plow and subsoil layer is captured by the inclusion of the interface term, $\mathrm{SOC}_{\mathrm{int}}$, which is determined by a piecewise equation that depends on whether the landscape is degrading or aggrading:

$$\mathrm{SOC}_{\mathrm{int}} = \begin{cases} \mathrm{SOC}|_{z=\eta-L_p} & \frac{\partial\eta}{\partial t} < 0 \\ \mathrm{SOC}_p & \frac{\partial\eta}{\partial t} > 0 \end{cases} \tag{4}$$

where z is the vertical coordinate. When the landscape degrades ($\partial\eta/\partial t < 0$), soil and SOC in the upper region of the subsoil are incorporated into the plow layer. When the landscape aggrades ($\partial\eta/\partial t > 0$), soil and SOC from the plow layer are buried and incorporated into the subsoil. The version of LEM-SOC originally reported by Kwang, Thaler, Quirk, et al. (2022) utilized a vertical grid that tracked the 3-dimensional evolution of SOC. However, it is not necessary to track the 3-dimensional evolution of SOC for our regionwide analysis nor is it computationally efficient. Therefore, we modified the original LEM-SOC model to make regionwide predictions. Details about the numerical implementation can be found in Text S2 in Supporting Information S1.

Due to the closed boundary conditions for the model, soil does not leave the domain, and the volume of eroded and deposited soil are equal. Hence to evaluate the magnitude and rate of soil and SOC redistribution, our analysis focuses on two parts of the landscape; erosional areas with convex-upward topography and areas where soil is deposited and buried, which have concave-upward topography (Figure 2a). The buried SOC mass is defined as the SOC that is deposited via tillage and is beneath the plow layer (Figure 2a) and is equal to the sum of the

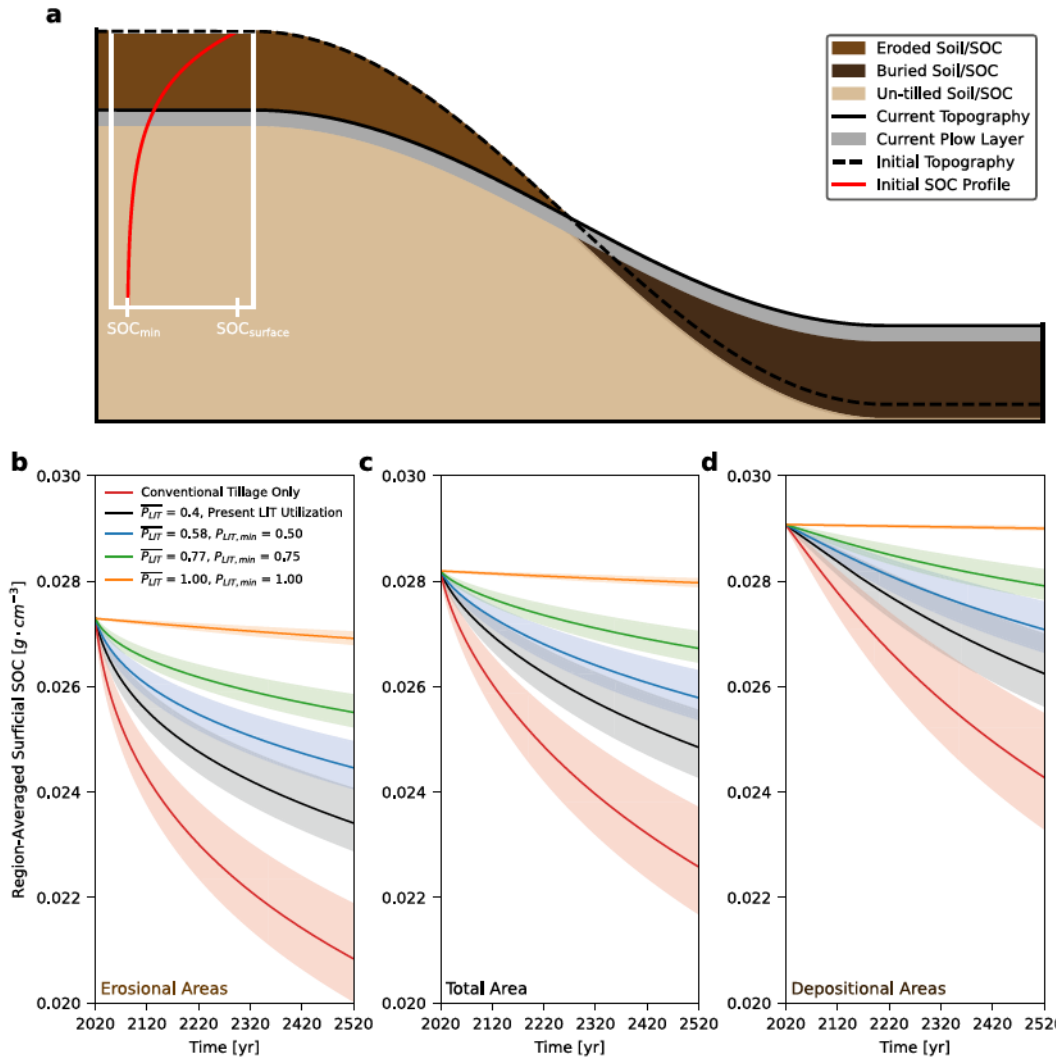

Figure 2. Diagram that depicts an idealized cross-section of Midwestern United States topography and soil organic carbon (SOC) distribution (a). The medium-dark brown and dark brown areas represent soil and SOC that have been eroded and buried, respectively. The white inset plot with the red line shows a typical initial SOC distribution where SOC decreases with depth. Time series showing region-averaged surficial SOC in the erosional (b), total (c), and depositional area (d), using $D = 0.5\ m^2 \cdot yr^{-1}$ and $D_{LIT} = 0.005\ m^2 \cdot yr^{-1}$. The red line represents a scenario where conventional tillage is employed across the entire region. The black line shows the present-day county level use of low-intensity tillage (Figure 1b). The blue, green, and orange lines display three different scenarios where a minimum proportion of low-intensity tillage, $P_{LIT,min}$, is specified (0.50, 0.75, 1.00, respectively). For each line, an envelope represents ranges of D (0.33–0.67 $m^2 \cdot yr^{-1}$) and D_{LIT} (0.0033–0.0067 $m^2 \cdot yr^{-1}$).

eroded SOC mass and the change in SOC mass within the plow layer in the depositional area (see Text S2 in Supporting Information S1).

3.3. Region-Scale Simulations

Across 403 counties that span 10 states, we employ LEM-SOC to forecast landscape evolution and SOC redistribution. We first estimate the reduction in soil and SOC redistribution by the current use of low-intensity tillage, relative to a hypothetical situation where the entire study area was farmed using conventional tillage. We then forecast how increasing the proportion of farmland employing low-intensity tillage would alter the redistribution of soil and SOC.

Compilations of soil transport coefficients for conventional tillage have a consistent and narrow range of 400–800 $kg \cdot m^{-1} \cdot yr^{-1}$ when the topographic gradient is calculated using the tangent of slope (or equivalently,

4–8 kg · m^{-1} · yr^{-1} · %$^{-1}$ when the topographic gradient is calculated using percent slope) (Lobb et al., 1995, 1999; Van Muysen et al., 2006; Van Oost et al., 2006). This range of soil transport coefficients represents soil erosion that occurs from a typical sequence of tillage operations (Van Oost et al., 2006). Govers et al. (1994) related the tillage coefficient to landscape evolution with the following equation (modified to be 2-dimensional):

$$\rho_b \frac{\partial \eta}{\partial t} = k_{\text{till}} \nabla^2 \eta \tag{5}$$

where ρ_b is a bulk density, and k_{till} is a tillage coefficient. By comparing Equation 1 with Equation 5, the value of D, in units of m^2 · yr^{-1}, is the quotient of the tillage transport coefficient and the soil bulk density. A value of 1,200 kg · m^{-3} is the median bulk density value from the USDA Rapid Carbon Assessment (RaCA) samples within our study area (Soil Survey Staff, 2013; Wills et al., 2014). Dividing the upper and lower values of published tillage transport coefficients (400–800 kg · m^{-1} · yr^{-1}) by bulk density (1,200 kg · m^{-3}), yields D values that range from 0.33 to 0.67 m^2 · yr^{-1} with $D = 0.5$ m^2 · yr^{-1} as the center value. We use the center value of $D = 0.5$ m^2 · yr^{-1} for our simulations and quantify the uncertainty of our prediction using the range of D (0.33–0.67 m^2 · yr^{-1}). We use a plow layer thickness, $L_p = 0.2$ m, the median thickness of the A_p (plowed A horizon) for 140 soil profiles located in the Western Corn Belt Plains Level III ecoregion (US EPA, 2015) from the RaCA data set (Soil Survey Staff, 2013). Although L_p varies from 0.06 to 0.38 m, we use $L_p = 0.2$ m because the results of LEM-SOC are insensitive to values within this range (Kwang, Thaler, Quirk, et al., 2022).

Roughly 40% of our study area (Figure 1a) contained fields that are currently farmed using low-intensity tillage (Azzari et al., 2019; Claassen et al., 2018), where using a D value for conventional tillage is inappropriate. Therefore, we use a diffusion coefficient that describes low-intensity tillage, D_{LIT}, for these areas. Low-intensity tillage includes strip-till and no-till practices, but the majority (~95%) of the areas with low-intensity tillage are farmed using no-till practices (Azzari et al., 2019). Measurements indicate soil transport coefficients for no-till are at least 2 orders of magnitude lower (<5 kg · m^{-1} · yr^{-1}) than coefficients for conventional tillage (Mollinedo, 2008; Petr & Josef, 2018). For simplicity, we simulate soil transport for no-till farming using a value of 6 kg · m^{-1} · yr^{-1} (tangent of slope) or 0.06 kg · m^{-1} · yr^{-1} · %$^{-1}$ (percent slope), which corresponds to $D_{\text{LIT}} = 0.005$ m^2 · yr^{-1}. In addition, we compute uncertainty in our predictions with a range of D_{LIT} that corresponds to D (0.0033–0.0067 m^2 · yr^{-1}). Because no-till is the predominant low-intensity tillage technique, we apply D_{LIT} to all areas that are classified as using as low-intensity tillage.

We determine tillage erosion for each county in our study area (Figure 1) using soil transport coefficients for both conventional ($D = 0.5$ m^2 · yr^{-1}) and low-intensity tillage ($D_{\text{LIT}} = 0.005$ m^2 · yr^{-1}). For each county, we estimate the county-averaged statistics, for example, total volume of soil eroded, mass of SOC eroded, mass of SOC buried, and change in surficial SOC stocks (see Text S2 in Supporting Information S1). We simulate the extent of low-intensity tillage in each county by specifying the proportion of the cultivated land area that uses low-intensity tillage, P_{LIT}, using data from Azzari et al. (2019) (Figure 1b). For each simulation, we estimate the county-averaged statistics and assume that they are an area-weighted sum of the conventional tillage and low-intensity tillage simulations.

$$X(t) = (1 - P_{\text{LIT}})X_T(t) + P_{\text{LIT}}X_{\text{LIT}}(t) \tag{6}$$

where X is the county-averaged statistic, P_{LIT} is the area proportion that uses low-intensity tillage, X_T is the county-averaged statistic from the tillage simulation, and X_{LIT} is the county-averaged statistic from the low-intensity tillage simulation. We simulate scenarios where the use of low-intensity tillage is increased by imposing a minimum area-proportion value of low-intensity tillage, $P_{\text{LIT,min}}$. For a given value of $P_{\text{LIT,min}}$, we use the original P_{LIT} values in counties where $P_{\text{LIT}} \geq P_{\text{LIT,min}}$ and increase the P_{LIT} to $P_{\text{LIT,min}}$ in counties where $P_{\text{LIT}} < P_{\text{LIT,min}}$.

The masks used for preprocessing the DEM remove some areas that are actively farmed, resulting in an underestimate of the total amount of soil and SOC redistribution. To reintegrate these areas to our estimate without reintroducing error from topographic anomalies, we multiply each county-averaged result by the ratio of the area that is categorized as Herbaceous Agriculture (Jennings, 2000) and the area that has the preprocessing filters applied. This calculation assumes that the landscape in the filtered area evolves similarly to the rest of the county. For our entire region of interest, the Herbaceous Agriculture area with the filter applied is 3.52×10^5 km^2 and the Herbaceous Agriculture Area is 4.01×10^5 km^2, for a regionwide ratio of 1.14.

3.4. Historical Soil Erosion and SOC Redistribution

Lastly, to determine how much soil and SOC have already been redistributed, field-scale (<1 km^2) simulations were conducted to compare historical (1860–2020) and future (2020–2520) agricultural erosion. We study three field sites (Hoffman, Stinson, Willis) (Figure 1a) in northern Iowa, where pre-agricultural (~1860) topographic and SOC conditions have been reconstructed (Kwang, Thaler, Quirk, et al., 2022). Using the reconstructions, we simulate tillage erosion at the Hoffman, Stinson, and Willis sites using a plow depth, L_p, = 0.2 m and $D = 0.21$, 0.40, 0.14 $m^2 \cdot yr^{-1}$, respectively, from 1860–2520. These D values were independently estimated for each site (Kwang, Thaler, Quirk, et al., 2022). We refer to this set of simulations as the Reconstruction Case. In addition, we ran a set of simulations where the initial pedostratigraphy at each site was generated from the gSSURGO data set, named the gSSURGO Case. We assume that gSSURGO represents the present-day pedostratigraphy and simulate soil and SOC redistribution from 2020–2520. Between 2020–2520, we assessed how well the two cases agree (Figures S1 and S2 in Supporting Information S1). Further details regarding the reconstruction can be found in Text S1 in Supporting Information S1.

We simulated an additional scenario to account for the transition from non-mechanized to mechanized agriculture that occurred in the early 20th century (see Text S1 in Supporting Information S1). The calibrated values of D from Kwang, Thaler, Quirk, et al. (2022) are lower than the D values compiled by Van Oost et al. (2006) because they average over a time period (1860–2020) that includes non-mechanized tillage with draft animals, rather than tractors (Kwang, Thaler, Quirk, et al., 2022), and soil transport coefficients for non-mechanized tillage are generally lower than mechanized tillage values (Van Oost et al., 2006). Since future soil transport by tillage at these three field sites may be underestimated by the D values calibrated with historical data, we ran a set of simulations that has a step increase in D to 0.50 $m^2 \cdot yr^{-1}$ after 2020 to simulate mechanized tillage.

4. Results

4.1. Conventional Tillage Only

By simulating conventional tillage across the entire region, we quantify a hypothetical maximum soil erosion rate for the Midwest. Furthermore, by comparing results from the conventional tillage-only simulation with a simulation based on the present-day low-intensity tillage use, we determine the current effectiveness of low-intensity tillage in reducing regionwide erosion. The initial average SOC concentration in the plow layer from the gSURRGO data set, which we term the surficial SOC, is 0.028 $g \cdot cm^{-3}$ (Figure 2c) and the concentrations are lower in erosional versus depositional areas (0.027 vs. 0.029 $g \cdot cm^{-3}$, respectively, Figures 2b and 2d). With time, our model predicts that the surficial SOC decreases across the entire landscape (Figure 2c) as well as in both erosional (Figure 2b) and depositional (Figure 2d) areas. With only conventional tillage, we predict the region-integrated surficial SOC concentration will decline by 7.6% (+1.6/−1.8%) in the next 100 years (Table 1). We also find that erosional areas experience a greater SOC reduction, and the depositional areas have a smaller SOC reduction than the entire region combined (Table 1).

In the entire region, the gSSURGO data set indicates there is 7.31 Pg of SOC in the uppermost 2-m of soil. If the entire landscape were to be tilled conventionally, we estimate that 3.9% (+0.7%/−0.8%) and 4.6% (+0.9%/−1.0%) of the total SOC stock would erode and be buried in the next 100 years (Table 2; Figures 3a and 3b), respectively. SOC is only a fraction of the soil mass transported by tillage, and correspondingly, soil erosion is estimated to be 17 ± 4 Pg in the next 100 years (Table 3; Figure 4a). The rates of SOC and soil redistribution are unsteady during the simulation; the rates of SOC erosion and burial quickly decelerate (Figures 3c and 3d). For example, the inset images in Figures 3c and 3d show that rates of erosion and burial more than halve within the first 25 years of the simulation. Initial region-averaged rates of SOC erosion and burial are 21 ± 7 and 22 ± 7 $g \cdot m^{-2} \cdot yr^{-1}$, respectively, but quickly decelerate (Table 2; Figures 3c and 3d). Region-averaged soil erosion rates are initially 2.2 ± 0.7 $kg \cdot m^{-2} \cdot yr^{-1}$, but also decelerate throughout the simulation (Table 3; Figure 4b).

4.2. Present-Day Use of Low-Intensity Tillage

Future estimates of soil and SOC erosion are lower than predicted by the scenario with conventional tillage only, because roughly 40% of the agricultural land area of the Midwestern U.S. is farmed with low-intensity tillage (Azzari et al., 2019) (Figure 1b). Under current use of low-intensity tillage, we predict there will be a

Table 1
Regionwide Surficial (0–20 cm) Soil Organic Carbon (SOC) Loss

Time[a] (yr)	Conventional tillage	Present-day LIT use	$P_{LIT,min} = 0.5$	$P_{LIT,min} = 0.75$	$P_{LIT,min} = 1$
SOC surface loss, negative curvature region (%)					
25	4.8% (+1.0/−1.2%)	2.7% (+0.6/−0.7%)	1.9% (+0.4/−0.5%)	1.2% (+0.3/−0.3%)	0.08% (+0.03/−0.03%)
50	7.4% (+1.4/−1.7%)	4.2% (+0.8/−1.0%)	3.0% (+0.6/−0.7%)	1.8% (+0.4/−0.4%)	0.16% (+0.05/−0.05%)
100	11.0% (+1.8/−2.2%)	6.4% (+1.1/−1.3%)	4.6% (+0.8/−1.0%)	2.8% (+0.5/−0.6%)	0.31% (+0.10/−0.10%)
250	17% (+2/−3%)	10.3% (+1.5/−1.9%)	7.5% (+1.1/−1.4%)	4.6% (+0.7/−0.9%)	0.7% (+0.2/−0.2%)
500	24% (+3/−4%)	14.2% (+1.9/−2.4%)	10.4% (+1.4/−1.8%)	6.5% (+1.0/−1.2%)	1.4% (+0.4/−0.4%)
SOC surface loss, full region (%)					
25	2.9% (+0.7/−0.8%)	1.6% (+0.4/−0.4%)	1.2% (+0.3/−0.3%)	0.69% (+0.17/−0.19%)	0.045% (+0.015/−0.015%)
50	4.8% (+1.0/−1.2%)	2.7% (+0.6/−0.7%)	1.9% (+0.4/−0.5%)	1.2% (+0.3/−0.3%)	0.09% (+0.03/−0.03%)
100	7.6% (+1.6/−1.8%)	4.4% (+0.9/−1.1%)	3.1% (+0.7/−0.8%)	1.9% (+0.4/−0.5%)	0.18% (+0.06/−0.06%)
250	14% (+3/−3%)	7.9% (+1.5/−1.8%)	5.7% (+1.1/−1.3%)	3.4% (+0.7/−0.8%)	0.43% (+0.13/−0.13%)
500	20% (+3/−4%)	12% (+2/−3%)	8.5% (+1.4/−1.8%)	5.2% (+0.9/−1.1%)	0.8% (+0.2/−0.2%)
SOC surface loss, positive curvature region (%)					
25	1.2% (+0.4/−0.4%)	0.6% (+0.2/−0.2%)	0.46% (+0.15/−0.14%)	0.27% (+0.09/−0.09%)	0.013% (+0.004/−0.004%)
50	2.3% (+0.7/−0.8%)	1.2% (+0.4/−0.4%)	0.9% (+0.3/−0.3%)	0.53% (+0.17/−0.17%)	0.03% (+0.01/−0.01%)
100	4.4% (+1.3/−1.4%)	2.4% (+0.8/−0.8%)	1.8% (+0.6/−0.6%)	1.0% (+0.3/−0.3%)	0.053% (+0.018/−0.018%)
250	10% (+3/−3%)	5.7% (+1.5/−1.7%)	4.0% (+1.1/−1.2%)	2.4% (+0.6/−0.7%)	0.13% (+0.04/−0.04%)
500	17% (+3/−4%)	10% (+2/−3%)	6.8% (+1.4/−1.8%)	4.0% (+0.8/−1.0%)	0.25% (+0.08/−0.08%)

[a]Time from present (2020).

4.4% (+0.9/−1.1%) decline in surficial SOC in the next 100 years (Table 1; Figure 2). Hence, we predict that the current implementation of low-intensity tillage will nearly halve the loss of surficial SOC relative to the hypothetical scenario where the entire landscape is farmed using conventional tillage.

The application of low-intensity tillage reduces the total amount and pace of soil (Table 3; Figure 4a) and SOC redistribution (Table 2; Figures 3a and 3b). The region-integrated SOC erosion is estimated to be 0.17 (+0.03/−0.04) Pg, and SOC burial is estimated to be 0.20 (+0.04/−0.05) Pg after 100 years. The total amount of soil erosion is also reduced to 8.8 (+1.9/−2.1) Pg after 100 years. Therefore, we estimate that the current use of low-intensity tillage will prevent 48% of soil erosion and 41% of SOC redistribution compared to simulations using the hypothetical case with only conventional tillage in the next 100 years. Furthermore, the model predicts that region-averaged SOC redistribution rates (Table 2; Figures 3c and 3d) and soil erosion rates (Table 3; Figure 4b) are approximately half the rates of those from the simulation that assumes only conventional tillage. We find initial rates of SOC erosion to be 12 ± 4 g $\cdot$ m^{-2} $\cdot$ yr^{-1}, and soil erosion rates to be 1.1 ± 0.4 kg $\cdot$ m^{-2} $\cdot$ yr^{-1}.

4.3. Increased Use of Low-Intensity Tillage

Soil and SOC erosion can be further reduced by increasing the implementation of low-intensity tillage. We simulated wider use of low-intensity tillage by increasing the minimum proportion of that land area of each county with low-intensity tillage to 0.50, 0.75, 1.00 ($P_{LIT,min}$) (Table 1). Increasing low-intensity tillage to $P_{LIT,min} = 0.50$ and $P_{LIT,min} = 0.75$, will result in a 30% and 57% reduction in surficial SOC loss after 100 years, respectively. If low-intensity tillage is used on all the cultivated acreage in the Midwestern U.S. ($P_{LIT,min} = 1.00$), it would prevent 96% of the surficial SOC loss predicted to occur relative to the current use of low-intensity tillage after 100 years.

As expected, increasing the application of low-intensity tillage also reduces predictions of SOC erosion and burial (Table 2; Figures 3a and 3b). By converting the entire region to low-intensity tillage, SOC redistribution (both erosion and burial) is decreased by 95% and 96% after 100 years, respectively. Similarly, total soil erosion is also

Table 2
Regionwide Soil Organic Carbon (SOC) Erosion and Burial: Cumulative Amount and Instantaneous Rates

Time[a] (yr)	Conventional tillage	Present-day LIT use	$P_{LIT,min} = 0.5$	$P_{LIT,min} = 0.75$	$P_{LIT,min} = 1$
Cumulative SOC erosion (Pg)					
25	0.12 (+0.03/−0.03)	0.070 (+0.015/−0.017)	0.050 (+0.011/−0.012)	0.030 (+0.006/−0.007)	0.0022 (+0.0007/−0.0007)
50	0.19 (+0.04/−0.04)	0.11 (+0.02/−0.03)	0.078 (+0.015/−0.018)	0.047 (+0.009/−0.011)	0.0043 (+0.0014/−0.0014)
100	0.29 (+0.05/−0.06)	0.17 (+0.03/−0.04)	0.12 (+0.02/−0.03)	0.072 (+0.014/−0.016)	0.008 (+0.003/−0.003)
250	0.47 (+0.07/−0.09)	0.28 (+0.05/−0.06)	0.20 (+0.03/−0.04)	0.13 (+0.02/−0.03)	0.020 (+0.006/−0.006)
500	0.66 (+0.08/−0.12)	0.40 (+0.06/−0.07)	0.29 (+0.04/−0.05)	0.18 (+0.03/−0.04)	0.036 (+0.010/−0.011)
Cumulative SOC burial (Pg)					
25	0.14 (+0.03/−0.03)	0.076 (+0.017/−0.020)	0.055 (+0.012/−0.014)	0.033 (+0.007/−0.008)	0.0022 (+0.0007/−0.0007)
50	0.22 (+0.05/−0.05)	0.12 (+0.03/−0.03)	0.088 (+0.019/−0.021)	0.053 (+0.011/−0.013)	0.0044 (+0.0014/−0.0014)
100	0.34 (+0.07/−0.08)	0.20 (+0.04/−0.05)	0.14 (+0.03/−0.03)	0.084 (+0.017/−0.020)	0.009 (+0.003/−0.003)
250	0.58 (+0.10/−0.12)	0.35 (+0.06/−0.08)	0.25 (+0.05/−0.05)	0.15 (+0.03/−0.03)	0.021 (+0.006/−0.007)
500	0.85 (+0.13/−0.16)	0.51 (+0.08/−0.10)	0.37 (+0.06/−0.07)	0.23 (+0.04/−0.05)	0.038 (+0.011/−0.012)
Instantaneous SOC erosion rate ($g \cdot m^{-2} \cdot yr^{-1}$)					
0	22 (+7/−7)	12 (+4/−4)	9 (+3/−3)	5.1 (+1.7/−1.7)	0.22 (+0.07/−0.07)
25	8.2 (+1.3/−1.6)	4.8 (+0.8/−1.0)	3.4 (+0.6/−0.7)	2.1 (+0.4/−0.4)	0.22 (+0.07/−0.07)
50	5.9 (+0.9/−1.1)	3.5 (+0.6/−0.7)	2.5 (+0.4/−0.5)	1.5 (+0.3/−0.3)	0.21 (+0.07/−0.06)
100	4.1 (+0.6/−0.8)	2.5 (+0.4/−0.5)	1.8 (+0.3/−0.4)	1.11 (+0.18/−0.22)	0.20 (+0.06/−0.06)
250	2.4 (+0.2/−0.4)	1.50 (+0.16/−0.23)	1.10 (+0.13/−0.18)	0.70 (+0.09/−0.12)	0.18 (+0.05/−0.05)
500	1.49 (+0.08/−0.15)	0.93 (+0.06/−0.10)	0.70 (+0.05/−0.08)	0.46 (+0.05/−0.07)	0.15 (+0.03/−0.04)
Instantaneous SOC burial rate ($g \cdot m^{-2} \cdot yr^{-1}$)					
0	22 (+7/−7)	12 (+4/−4)	9 (+3/−3)	5.2 (+1.7/−1.7)	0.22 (+0.07/−0.07)
25	9.6 (+1.8/−2.1)	5.5 (+1.1/−1.2)	3.9 (+0.8/−0.9)	2.4 (+0.5/−0.5)	0.22 (+0.07/−0.07)
50	7.1 (+1.3/−1.5)	4.2 (+0.8/−0.9)	3.0 (+0.6/−0.7)	1.8 (+0.4/−0.4)	0.21 (+0.07/−0.07)
100	5.3 (+0.9/−1.1)	3.2 (+0.6/−0.7)	2.3 (+0.4/−0.5)	1.4 (+0.3/−0.3)	0.21 (+0.06/−0.07)
250	3.3 (+0.4/−0.6)	2.0 (+0.3/−0.4)	1.5 (+0.2/−0.3)	0.91 (+0.13/−0.17)	0.19 (+0.05/−0.06)
500	2.12 (+0.15/−0.26)	1.32 (+0.11/−0.18)	0.97 (+0.09/−0.14)	0.62 (+0.07/−0.10)	0.17 (+0.04/−0.05)

[a]Time from present (2020).

reduced by 95% after 100 years (Table 3; Figure 4a). The corresponding region-averaged rates of SOC erosion and burial are dramatically lower with the increased application of low-intensity (Table 2; Figures 3c and 3d). If low-intensity tillage is applied across the entire region, we calculate initial rates of SOC erosion, SOC burial, and soil erosion (Table 3; Figure 4b) would all be 98% less than the estimate based on current tillage trends.

4.4. Regional Distribution of SOC Erosion

Maps of county-integrated predictions reveal the areas with the greatest rates and amount of SOC redistribution (Figure 5). The simulation that assumes only conventional tillage depicts a relatively even spatial distribution of SOC erosion (Figure 5a). Under current use in low-intensity tillage, SOC erosion over the next 100 years is greatest in counties that are north of the Last Glacial Maximum (LGM) ice margin (Figure 5b), where SOC (Figure 1a) and use of conventional tillage (Figure 1b) is high. If $P_{LIT,min} = 0.50$, counties north of the LGM in Figure 4b experience a decrease in SOC erosion while the SOC erosion in the counties south of the LGM ice margin are mostly unchanged (Figure 5c). This occurs because P_{LIT} in most of the counties south of the LGM already exceeds 0.50. Reductions in SOC erosion are predicted to occur throughout the Midwestern U.S. when $P_{LIT,min}$ is equal to 0.75 (Figure 5d) and 1.00 (Figure 5e). The spatial distributions of county-integrated soil erosion, surficial SOC reduction, and SOC erosion after 100, 300, and 500 years are shown in Figures S3–S5 in Supporting Information S1.

10.1029/2022EF003104

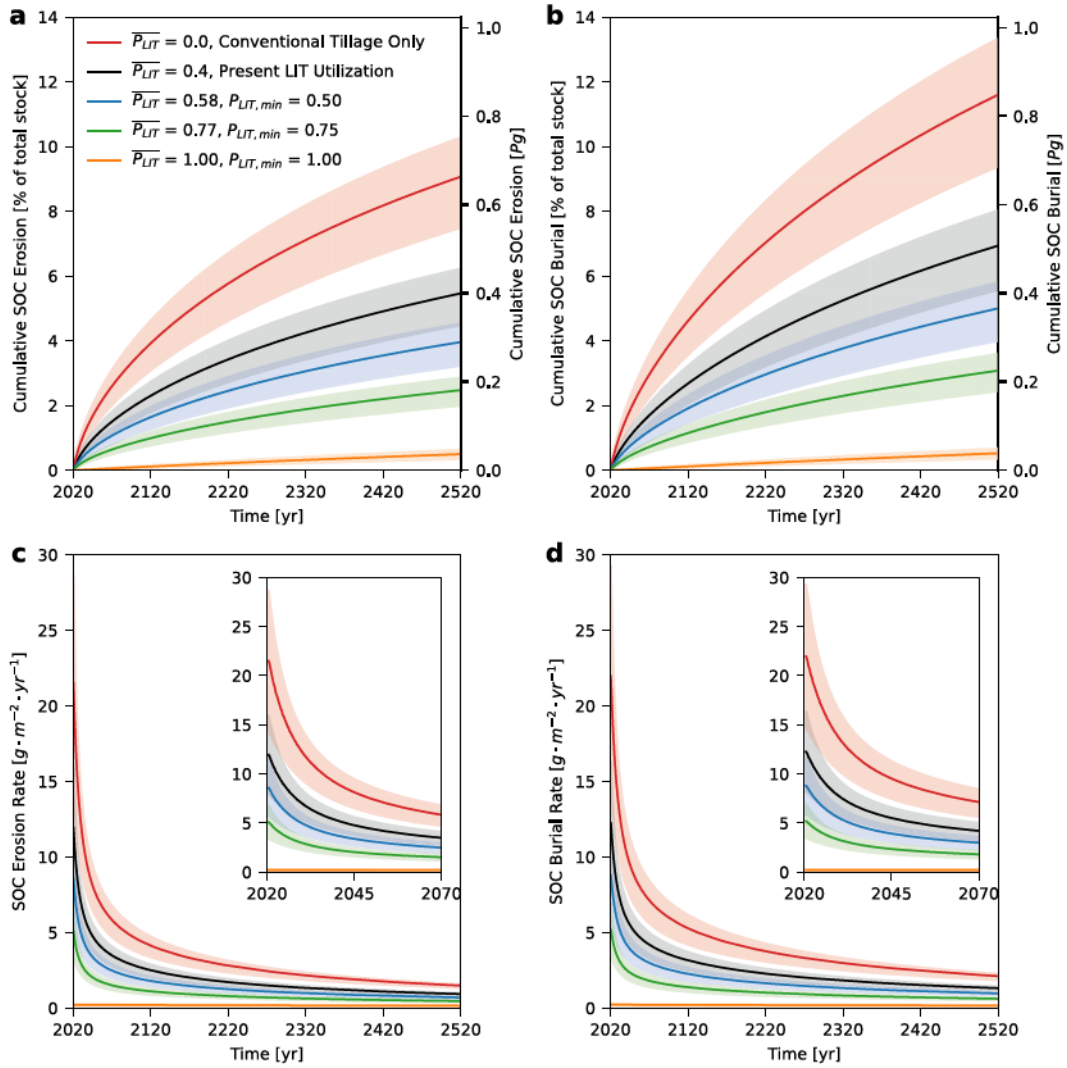

Figure 3. Regionwide integrated time series of total soil organic carbon (SOC) erosion (a) and burial (b) using $D = 0.5\ m^2 \cdot yr^{-1}$ and $D_{LIT} = 0.005\ m^2 \cdot yr^{-1}$. The red line shows results from a hypothetical situation where all farms use conventional tillage. The black line shows results from the simulation that assumes the present-day use of low-intensity tillage (Figure 1b). The blue, green, and orange lines are results from simulations where $P_{LIT,min}$ values of 0.50, 0.75, and 1.00 are specified, respectively. The corresponding envelopes for each line represent ranges of D (0.33–0.67 $m^2 \cdot yr^{-1}$) and D_{LIT} (0.0033–0.0067 $m^2 \cdot yr^{-1}$). The corresponding SOC erosion rates (c) and SOC burial rates (d) are normalized by area. The inset plots show an expanded view of the rates between 2020–2070.

4.5. Historical Soil Erosion and SOC Redistribution

Simulations that estimate SOC redistribution from the time of European settlement (1860) to 500 years in the future (2520) predict that the total amount of erosion over the next 500 years will be of the same order as the amount of erosion that occurred during the past 160 years at our three field sites in Iowa (Figure 6). Patterns of SOC redistribution (Figures S6–S8 in Supporting Information S1) and total SOC erosion and burial (Figure 6) agree well between the Reconstruction Case and gSSURGO Case. From 1860–2520, we estimate SOC erosion to range from 2.3 to 3.1 $kg \cdot m^{-2}$ and SOC burial to range from 3.1 to 4.4 $kg \cdot m^{-2}$ (Figure 6). Over the 660-year simulation, 45%–52% of SOC erosion and 40%–47% of SOC burial occur between 1860–2020. Although a large portion of SOC has been lost from upper soil horizons (Thaler et al., 2021, 2022), there is still SOC that is vulnerable to future erosion. Between 1860–2020, surficial SOC declines by 12%–15%, and between 2020 and 2520, it declines by 16%–26% (Figure S9a in Supporting Information S1). Therefore, between 37% and 48% of the surficial SOC loss predicted to occur from the start of farming to 500 years in the future has already occurred.

Table 3
Regionwide Soil Erosion: Cumulative Amount, Instantaneous Mass Rate, and Instantaneous Volume Rate

Time[a] (yr)	Conventional tillage	Present-day LIT use	$P_{LIT,min} = 0.5$	$P_{LIT,min} = 0.75$	$P_{LIT,min} = 1$
Cumulative soil erosion (Pg)					
25	6.5 (+1.5/−1.7)	3.3 (+0.8/−0.9)	2.5 (+0.6/−0.7)	1.5 (+0.4/−0.4)	0.10 (+0.03/−0.03)
50	11 (+2/−3)	5.5 (+1.2/−1.4)	4.1 (+0.9/−1.0)	2.6 (+0.6/−0.6)	0.21 (+0.07/−0.07)
100	17 (+4/−4)	8.8 (+1.9/−2.1)	6.6 (+1.4/−1.6)	4.2 (+0.9/−1.0)	0.41 (+0.13/−0.14)
250	31 (+6/−7)	16 (+3/−4)	12 (+3/−3)	7.7 (+1.6/−1.8)	1.0 (+0.3/−0.3)
500	48 (+9/−10)	25 (+5/−5)	19 (+4/−4)	12 (+2/−3)	1.9 (+0.5/−0.6)
Instantaneous mass-based soil erosion rate ($kg \cdot m^{-2} \cdot yr^{-1}$)					
0	2.2 (+0.7/−0.7)	1.1 (+0.4/−0.4)	0.8 (+0.3/−0.3)	0.50 (+0.16/−0.16)	0.021 (+0.007/−0.007)
25	0.98 (+0.19/−0.22)	0.50 (+0.10/−0.11)	0.38 (+0.08/−0.09)	0.23 (+0.05/−0.05)	0.021 (+0.007/−0.007)
50	0.75 (+0.15/−0.17)	0.39 (+0.08/−0.09)	0.29 (+0.06/−0.07)	0.18 (+0.04/−0.04)	0.021 (+0.007/−0.007)
100	0.57 (+0.11/−0.13)	0.30 (+0.06/−0.07)	0.23 (+0.05/−0.05)	0.14 (+0.03/−0.03)	0.020 (+0.006/−0.006)
250	0.40 (+0.07/−0.09)	0.21 (+0.04/−0.04)	0.16 (+0.03/−0.03)	0.103 (+0.019/−0.023)	0.018 (+0.005/−0.006)
500	0.29 (+0.04/−0.06)	0.15 (+0.02/−0.03)	0.117 (+0.018/−0.023)	0.077 (+0.013/−0.016)	0.016 (+0.004/−0.005)
Instantaneous volume-based soil erosion rate ($mm \cdot yr^{-1}$)					
0	1.8 (+0.6/−0.6)	0.9 (+0.3/−0.3)	0.7 (+0.2/−0.2)	0.41 (+0.14/−0.14)	0.018 (+0.006/−0.006)
25	0.81 (+0.16/−0.18)	0.42 (+0.08/−0.10)	0.31 (+0.06/−0.07)	0.20 (+0.04/−0.05)	0.018 (+0.006/−0.006)
50	0.62 (+0.12/−0.14)	0.32 (+0.07/−0.07)	0.24 (+0.05/−0.06)	0.15 (+0.03/−0.04)	0.017 (+0.006/−0.005)
100	0.48 (+0.09/−0.11)	0.25 (+0.05/−0.06)	0.19 (+0.04/−0.04)	0.12 (+0.03/−0.03)	0.017 (+0.005/−0.005)
250	0.33 (+0.06/−0.07)	0.17 (+0.03/−0.04)	0.13 (+0.02/−0.03)	0.086 (+0.016/−0.019)	0.015 (+0.004/−0.005)
500	0.24 (+0.04/−0.05)	0.125 (+0.018/−0.023)	0.098 (+0.015/−0.019)	0.064 (+0.010/−0.013)	0.014 (+0.003/−0.004)

[a]Time from present (2020).

The site-calibrated D values likely underestimate future tillage because they were calibrated over a period when the farms operated with both non-mechanized and mechanized tillage. Results from the simulations that account for the shift in mechanization show that total SOC erosion and burial increase to 2.9–4.0 and 4.2–6.0 $kg \cdot m^{-2}$, respectively (Figure S10 in Supporting Information S1). The historical SOC redistribution (1860–2020) makes up a smaller percentage of SOC redistribution throughout the entire simulation (28%–49% of SOC erosion and 25%–44% of burial) relative to the simulations that only use D values calibrated from historical data. In simulations that account for the transition to mechanization, surficial SOC declines by 18%–46% between 2020–2520 (Figure S9b in Supporting Information S1).

5. Discussion

Agriculture greatly accelerated soil erosion in the period following the initiation of farming. Our model predicts that the present-day region-averaged rate of soil erosion is 0.9 ± 0.3 $mm \cdot yr^{-1}$ or 1.1 ± 0.4 $kg \cdot m^{-2} \cdot yr^{-1}$ (which converts to 4.9 ± 1.8 $ton \cdot acre^{-1} \cdot yr^{-1}$) under current use of low-intensity tillage. Nearly half of this forecast range exceeds the maximum tolerable soil erosion rate for the region, which is 5.0 $tons \cdot acre \cdot yr^{-1}$ (U.S. Department of Agriculture, 2018). Under current use of low-intensity tillage, we predict 190 (+80/−130) out of 403 counties have county-averaged soil erosion rates that outpace this soil tolerance value. However, soil loss tolerance values are much too high to sustain soils, as rates of agricultural soil erosion in the Midwestern U.S. outpace soil production rates by orders of magnitude (Quarrier et al., 2022). Even after 100 years, our model predicts soil erosion rates will decelerate to 0.25 (+0.05/−0.06) $mm \cdot yr^{-1}$ or 0.30 (+0.06/−0.07) $kg \cdot m^{-2} \cdot yr^{-1}$ (which converts to 1.3 ± 0.3 $ton \cdot acre^{-1} \cdot yr^{-1}$) a rate that still outpaces soil production rates in the Midwestern U.S. (see Figure 2 in Quarrier et al., 2022).

The rapid initial rate of erosion is not permanent; the diffusive nature of tillage erosion causes the rate of soil erosion to decelerate over time (Figure 4). Because SOC flux is dependent on soil flux, we also predict a deceleration in

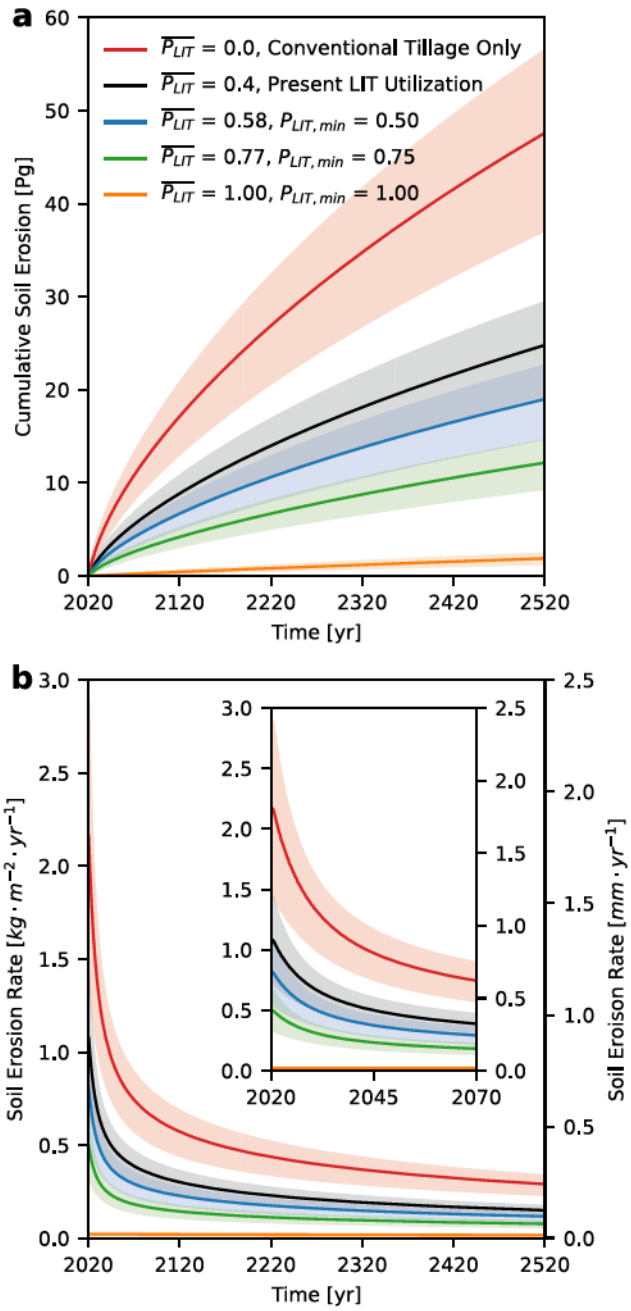

Figure 4. Total regionwide soil erosion assuming a bulk density of 1,200 kg · m^{-3}, $D = 0.5$ $m^2 \cdot yr^{-1}$ and $D_{LIT} = 0.005$ $m^2 \cdot yr^{-1}$ (a). The red line represents a simulation where all farms use conventional tillage. The black line shows the simulation that assumes the present-day county level use of low-intensity tillage (Figure 1b). The blue, green, and orange lines are results from simulations where $P_{LIT,min}$ values of 0.50, 0.75, and 1.00 are specified, respectively. The corresponding envelopes for each line represent ranges of D (0.33–0.67 $m^2 \cdot yr^{-1}$) and D_{LIT} (0.0033–0.0067 $m^2 \cdot yr^{-1}$). The corresponding soil erosion rates normalized by area (b). The inset plot shows an expanded view of the rates between 2020–2070.

SOC redistribution (Figure 3). In addition, SOC erosion decreases with time because surface SOC concentrations decline over time (Figure 2). As erosion occurs, the concentrations of SOC on the hilltops decrease because relatively low SOC soil from deeper in the profile is exhumed (Figure 2b). Because SOC flux is a product of soil flux and SOC concentration, a decrease in SOC concentration in the source material will also decelerate SOC redistribution. After 100 years, we predict rates of soil and SOC erosion to decrease by 73% (Figure 4b) and 79% (Figure 3), respectively, while surficial SOC concentration in the erosional areas decrease by 6.4% (+1.1/−1.3%) (Figure 2). Therefore, the deceleration in SOC erosion is dictated primarily by deceleration in soil erosion due to topographic diffusion, rather than reduction in SOC concentrations at the soil surface in eroding parts of the landscape.

Quantifying the impact of soil erosion on the global carbon cycle typically involves an assumption that the rate of soil and SOC redistribution is steady with time (Berhe et al., 2007; Doetterl et al., 2016; Kuhn et al., 2009; Lal, 2003; Van Oost et al., 2007). A decline in rates in SOC redistribution implies that the highest rates occurred in the past, shortly after the inception of agriculture (West et al., 2004). In our simulations of historical erosion, we estimate that the amount of SOC erosion from the time of European settlement of the Midwestern U.S. to the present (1860–2020) is roughly the same as the amount of SOC erosion forecasted to occur in the next 500 years (2020–2520). Our model results hence indicate that the influence of SOC redistribution on the global carbon cycle is time-dependent, with the largest potential for SOC burial taking place in regions where the initiation of farming has occurred more recently. In other regions, where plow-based agriculture has been implemented at much longer timescales, such as Eurasia and Africa (Lal et al., 2007), rates of SOC redistribution have had more time to decline. In contrast, SOC redistribution in North America has a greater potential to affect the global carbon cycle because relatively carbon-rich soils are being actively transported (Doetterl et al., 2016).

Our model results indicate that reducing erosion in the immediate future has the greatest potential to reduce SOC redistribution. By including the effects of landscape evolution, we find that agriculturally driven soil and SOC redistribution is temporally unsteady and is forecasted to substantially decrease with time (Figures 3 and 4). Hence, our results indicate that previous estimates of the impact of agricultural erosion on the global carbon cycle may only apply to the immediate future and that the potential for redistributing SOC via erosion or burial will diminish with time. Therefore, our results support those of Li et al. (2018), who concluded that to assess long-term changes in the global carbon cycle, estimates of SOC redistribution need to account for topographic dynamics and the effects of landscape evolution.

The region-averaged SOC erosion and burial rates at the at the start of the simulation (the present-day) are both 12 ± 4 g · m^{-2} · yr^{-1}. Though we do not assess the net C flux associated with soil redistribution, a value of 12 ± 4 g · m^{-2} · yr^{-1} exceeds 92.9% of previously reported positive and negative C fluxes for agricultural uplands, based on a compilation of results from field- to global-scale studies (Van Oost & Six, 2023). One of the 14 SOC fluxes compiled by Van Oost and Six (2023) that exceeded our result was estimated from a field within the Midwestern U.S. (22.4 g · m^{-2} · yr^{-1}; Manies et al., 2001). Hence, relative to the rest of the Earth, our results and those from prior work indicate the Midwestern U.S. is a hotspot for SOC erosion. The Midwestern U.S. is therefore a region where there is a high

10.1029/2022EF003104

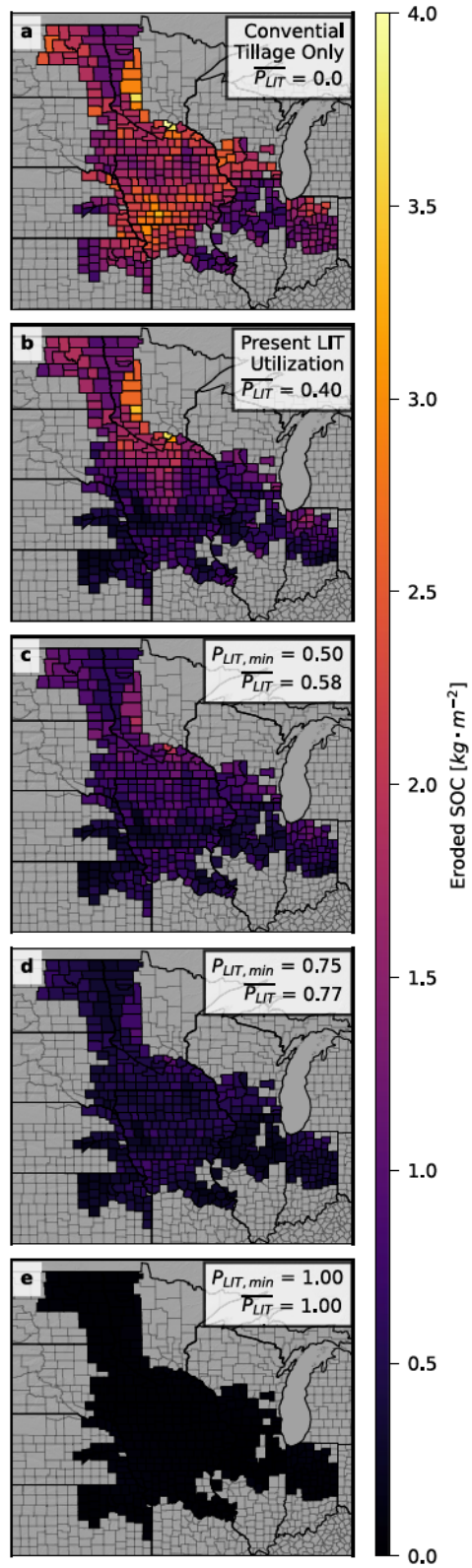

Figure 5. Map of county-averaged soil organic carbon (SOC) erosion after 100 years of simulated agricultural erosion from 2020–2120, using $D = 0.5\ m^2 \cdot yr^{-1}$ and $D_{LIT} = 0.005\ m^2 \cdot yr^{-1}$. Eroded mass of SOC per area is calculated by dividing the total mass of SOC in the eroded soil by the area that experiences erosion. SOC erosion is shown for the following scenarios: all farms are tilled conventionally (a), farms use present-day levels of low-intensity tillage (b), a value of $P_{LIT,min}$ of 0.50 is imposed so all counties have a P_{LIT} of at least 0.50 (c), $P_{LIT,min} = 0.75$ (d), and all farms use low-intensity tillage, that is, $P_{LIT,min} = 1.00$ (e).

10.1029/2022EF003104

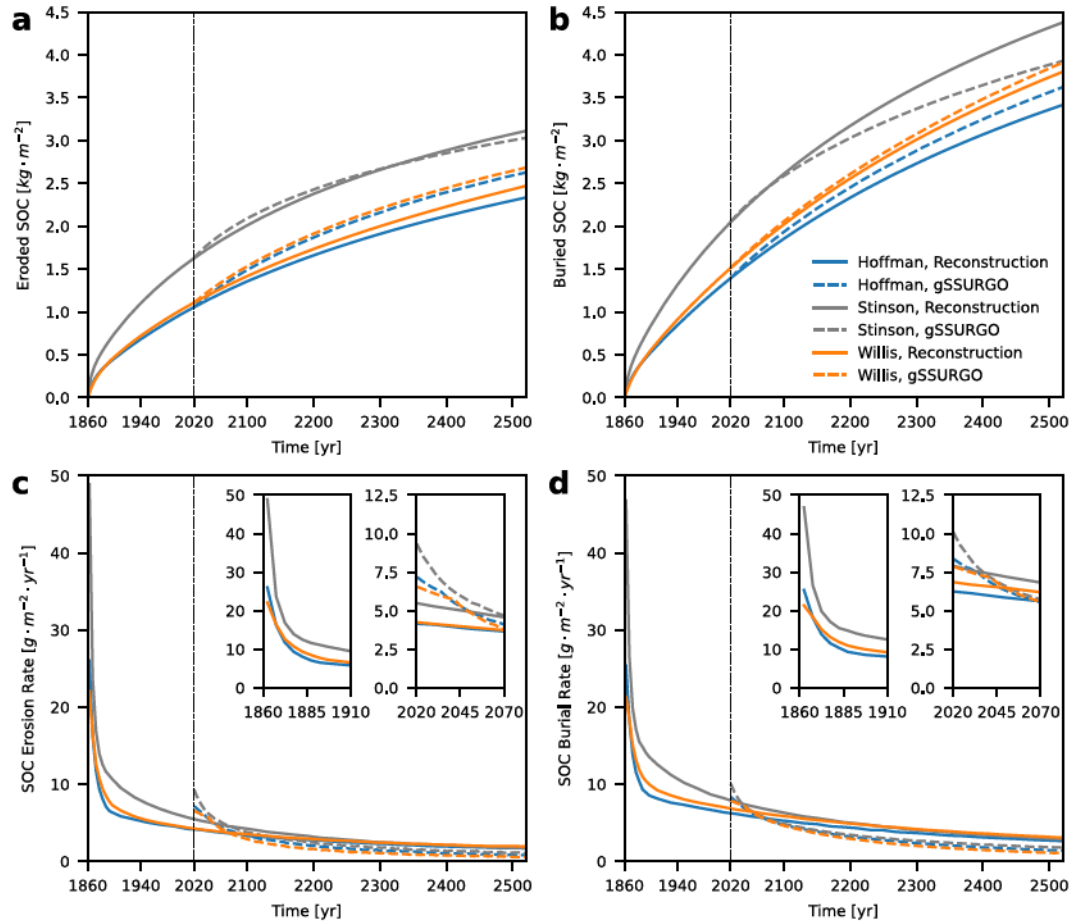

Figure 6. Soil organic carbon (SOC) erosion from 1860–2520 for the Hoffman, Stinson, and Willis field sites in Iowa (a). The solid lines show simulations from the Reconstruction Case (1860–2520) and the dashed lines show simulations from the gridded Soil Survey Geographic Database Case (2020–2520). Erosion is driven by D values of 0.21, 0.40, and 0.14 $m^2 \cdot yr^{-1}$ for the Hoffman, Stinson, and Willis sites, respectively. SOC burial from 1860–2520 (b). (c) and (d) depict the rates of SOC erosion and burial associated with (a) and (b), respectively. The inset images show expanded views of erosion and burial rates between 1860–1910 and 2020–2070.

potential for reducing the release of C to the atmosphere by implementation of practices that reduce soil redistribution and for generating a C sink via practices that return C to eroded soils.

Predictions of SOC redistribution in our model are only a function of SOC transport by diffusive tillage erosion. SOC dynamics such as mineralization/decomposition (Lal, 2003) and dynamic replacement (Harden et al., 1999) are not implemented in our model. As soil is eroded and transported on the surface of the landscape, mineralization of SOC can generate a source of atmospheric CO_2 (Lal, 2003). Our model indicates that the potential for mineralization may decline because SOC is buried, reducing decomposition (Berhe et al., 2007), and the surficial stock of SOC that is susceptible to decomposition decreases over time (Figures 2b and 2d). Dynamic replacement has the potential to increase carbon sequestration in soils (Berhe et al., 2007) by restoring SOC stocks in eroded soils. The inclusion of dynamic replacement in our model would increase the amount of eroded SOC because SOC concentration in the actively eroding areas would be partially replenished. However, dynamic replacement seems to play a small role compared to erosional SOC transport in the Midwestern U.S. because there is a widespread and persistent absence of A-horizon soils on the hilltops (Thaler et al., 2021, 2022), which indicates SOC loss via erosion far outpaces its replacement by crops. Additionally, Kwang, Thaler, Quirk, et al. (2022) found that the spatial pattern of SOC erosion can be reproduced by soil transport dynamics alone, which is also consistent with SOC reduction via soil erosion greatly outpacing dynamic replacement.

Unlike most soil erosion models (Arnold et al., 1998; Laflen et al., 1991; Renard et al., 1997; Van Oost et al., 2000; Wischmeier & Smith, 1978) that incorporate water erosion, LEM-SOC only simulates soil erosion via diffusive transport caused by tillage. In convex-upward regions, where small amounts of flow accumulate, the incorporation of water erosion does not significantly improve the prediction of SOC erosion (Kwang, Thaler, Quirk, et al., 2022). Whereas in topographic concavities where flow accumulates, water erosion has the potential to remove soils from the field to the stream network, decreasing SOC burial within fields. However, the majority of eroded soil is likely stored locally with fields (Blair et al., 2022; Stallard, 1998) because soil deposition due to agricultural erosion outpaces soil export via water erosion (Pennock & De Jong, 1987; Van Oost et al., 2000). Rill and gully erosion can also increase rates of hillslope erosion by drainage network expansion and local base-level lowering, but their effect would be small within our simulation's timescales (Text S3 in Supporting Information S1) (Fernandes & Dietrich, 1997). Importantly, water erosion can selectively transport fine-grained, low-density aggregates with high SOC content (Doetterl et al., 2016; Nadeu et al., 2012) that can lead to SOC enrichment in topographic depressions (Berhe et al., 2012; Gregorich et al., 1998; Quine & Oost, 2007). It is possible that our model only predicts net reductions in surficial SOC in depositional areas because it omits water erosion and selective transport. However, our model predictions are consistent with other studies that observe soil profile inversion caused by the burial of SOC-rich soils by relatively SOC-poor soils that are transported from the erosional areas (Kwang, Thaler, Quirk, et al., 2022; VandenBygaart, 2001; Yan et al., 2019). Nevertheless, our model predictions indicate that water erosion, also a function of slope (Laflen et al., 1991; Renard et al., 1997), will become less influential because topographic gradient decreases over time. In contrast, changes in the hydrologic cycle due to climate change have been predicted to increase water erosion in the future (Borrelli et al., 2020; O'Neal et al., 2005). Because those models assume a constant topographic gradient, they are most suitable for near-term predictions.

Historically, agricultural erosion is estimated to have resulted in 133 Pg of SOC loss globally, with rates of loss dramatically increasing in the past two centuries (Sanderman et al., 2017) due to an increase in the area of cultivation. Past SOC erosion has reduced crop yields, jeopardized global food security, and caused significant economic losses (Amundson et al., 2015; Montgomery, 2007a). To understand future stresses on crop yields, it is important to compare historical and future SOC erosion. Historical soil and SOC erosion in the Midwestern U.S. are estimated to be responsible for reducing crop yields by 6%, costing $2.8 billion annually (Thaler et al., 2021). We find that within 250–300 years, the forecasted surficial SOC loss (post-2020) will equal the historical surficial SOC loss (1860–2020) (Figure S9a in Supporting Information S1), but this initial analysis assumes steady D values that were calibrated to represent landscape evolution between 1860–2020 (Kwang, Thaler, Quirk, et al., 2022). Modern-day tillage operations are more intense (higher D or k_{till}) than historical methods due to the transition from non-mechanical to mechanical agricultural practices (Olmstead & Rhode, 2001; Van Oost et al., 2006). Therefore, calibrations of D from fields prepared with older, less intense tillage implements lead to conservative predictions of soil and SOC redistribution. By accounting for this transition, we find that the forecasted surficial SOC loss (post-2020) accelerates and will equal the historical surficial SOC loss (1860–2020) within 70–250 years (Figure S9b in Supporting Information S1). Although the mechanical power of tillage has increased in the past decades (Van Oost et al., 2006), tillage intensity has also been decreasing (lower D or k_{till}) because farmers have been transitioning from more aggresive implements (e.g., moldboard plow) to less aggressive implements (e.g., chisel plow, strip-till) in the last 50 years (De Jong-Hughes & Daigh, 2017). Because our scenarios assume a constant value of D, our forecasts of soil and SOC redistribution could be overestimations, especially if less-aggressive tillage impliments are more widely adopted in the future. However, D values for less aggressive tillage impliments are larger than values for non-mechanized tillage. Even if the less aggressive tillage impliments are used more widely, soil transport rates will still be greater than they were during the first several decades of non-mechanized farming. Hence we expect that future SOC loss will still equal historical values on similar, centennial timescales.

Because future predictions of surficial SOC loss are of similar magnitude to historical loss, we expect economic losses will continue to rise and that crop yields will further decline as the land area with SOC-poor soil expands (e.g., Figures S6–S8 in Supporting Information S1). With current low-intensity tillage use, we predict a 4.4% (+0.9/−1.1%) loss in surficial SOC in the next 100 years, but total regionwide implementation of low-intensity tillage can substantially decrease losses to only 0.18 ± 0.06%. Not only will further adoption of low-intensity tillage decelerate future increases in crop yield and economic losses, it may facilitate yield improvement and SOC replacement, if coupled with soil regenerative farming methods (Lal, 2006; Loisel et al., 2019; Montgomery, 2017; Montgomery et al., 2022).

Low-intensity tillage reduces both soil and SOC redistribution and decreases the burial of SOC-rich soils. We find that the current use of low-intensity tillage will prevent 0.17 (+0.03/−0.04) Pg of SOC erosion, 0.20 (+0.04/−0.05) Pg of SOC burial, and 8.8 (+1.9/−2.1) Pg of soil erosion over the next 100 years. If the Midwestern U.S. were only tilled conventionally, there would be 71% more SOC loss. Therefore, the application of low-intensity tillage is effective and a first-order farming practice that can reduce soil and SOC redistribution. We find that the total amount of SOC erosion, SOC burial, soil erosion, and surficial SOC loss would decrease between 95% and 96% in the next 100 years if the entire region were to adopt low-intensity tillage practices such as no-till farming. The subregion that would most benefit from the full adoption of low-intensity tillage is the area north of the LGM ice limit. This subregion has counties with the lowest use of low-intensity tillage (Figure 1b) but have the highest stocks of SOC (Figure 1a; Figure S11 in Supporting Information S1). Soils north of the LGM ice limit are tilled more often because the soils are heavy, fine-grained, and poorly drained (Azzari et al., 2019). But because these counties both heavily use conventional tillage and contain high SOC stocks (Figure 1), they are potential hotspots for reducing region-averaged soil and SOC erosion through incentivized soil conservation programs, such as the USDA Conservation Reserve Program (National Science and Technology Council, 2016).

Prior work has shown the efficacy of no-till farming methods in reducing soil erosion rates (Montgomery, 2007b). By simulating soil erosion and deposition, we have estimated—at the regional scale of the Midwestern U.S.—the magnitude by which wider adoption of no-till farming could reduce the transfer of SOC from hillslopes to depositional areas where it is buried. Burial of SOC and its replacement contribute to sequestration of atmospheric CO_2 (Berhe et al., 2007; Georgiou et al., 2022). Our findings and those of others suggest there has been substantial burial of SOC within the Midwestern U.S. (Li et al., 2018; Papiernik et al., 2009; Smith et al., 2001; Young et al., 2014). Given that a large extent of the Midwestern U.S. has soils where SOC stocks have been degraded (Thaler et al., 2021, 2022), there is potential to restore agricultural soils via regenerative practices (Montgomery, 2017; Schneider et al., 2021). Whether adoption of no-till farming can also return atmospheric SOC to soils is a matter of debate; field trials have shown that no-till farming can increase SOC (Kumar et al., 2012; West & Post, 2002) and regionwide studies and compilations have shown that no-till increases SOC in upper soil horizons (Christopher et al., 2009; Luo et al., 2010; Nunes et al., 2020). However, no-till may not necessarily increase SOC stock for the entire soil profile relative to conventional tillage (Christopher et al., 2009; Luo et al., 2010). Hence it has been advocated that no-till farming should be adopted primarily for soil sustainability benefits, rather than CO_2 sequestration (Powlson et al., 2014). However, there have been few studies that have assessed the role of soil regenerative agriculture, which includes no-till, but also planting cover crops and diverse crop rotations (Montgomery, 2017), on whole-profile SOC stocks (Montgomery et al., 2022), and such methods may result in more CO_2 sequestration than no-till alone.

6. Conclusion

We use a landscape evolution model to simulate agricultural soil erosion and SOC redistribution in the Midwestern U.S. over century timescales. Our model predicts that present-day region-averaged rates of soil and SOC erosion are 1.1 ± 0.4 and 12 ± 4 kg $\cdot$ m^{-2} $\cdot$ yr^{-1}, respectively. Nearly half of the uncertainty range of the predicted soil exceeds the maximum soil tolerance values for the region, and the SOC erosion rate outpaces most of the previously measured SOC fluxes in agricultural uplands (Van Oost & Six, 2023). Unlike other models, our landscape evolution modeling approach gives insight into how these rates will change in the future as topography and soil profiles evolve. Due to the diffusive nature of agricultural erosion, our model predicts that rates of soil and SOC redistribution will both decelerate.

Our findings also indicate that enhanced adoption of no-till farming has the potential to greatly reduce the erosion of soil and SOC. Regardless of any benefits for CO_2 sequestration, decreasing the rate of SOC redistribution will slow declines in crop yields caused by erosion and reduce the economic and environmental costs associated with soil erosion and the use of synthetic fertilizer to replace the function of degraded soils (Amundson et al., 2015; Montgomery, 2007b; Pimentel et al., 1995; Tilman et al., 2002). Because the fastest rates of soil redistribution due to tillage are occurring at present, and SOC concentrations in eroding soil are greater now than they will be in the future (Meersmans et al., 2009; Rosenbloom et al., 2001, 2006; Sulman et al., 2020), no-till farming will have a disproportionally larger impact on soil sustainability if it is adopted sooner, rather than later.

Data Availability Statement

County-level datafiles (Kwang, Thaler, & Larsen, 2022) are available through Scholarworks at UMass Amherst: https://doi.org/10.7275/tgmw-s318. The code files for the model (Kwang, 2022) can be found at https://doi.org/10.5281/zenodo.6647033.

Acknowledgments
The authors have no financial conflicts of interests to declare. This work was funded by the National Science Foundation (1653191) and the National Aeronautics and Space Administration (80NSSCK0747) grants to IJL. We would like to thank Azzari et al. (2019) for providing us with county-level estimates of low-intensity tillage use. We would also like to acknowledge Charlie Shobe and one anonymous reviewer for their valuable feedback and constructive reviews.

References

Amundson, R., Berhe, A. A., Hopmans, J. W., Olson, C., Sztein, A. E., & Sparks, D. L. (2015). Soil and human security in the 21st century. *Science*, *348*(6235), 1261071. https://doi.org/10.1126/science.1261071

Arnold, J. G., Srinivasan, R., Muttiah, R. S., & Williams, J. R. (1998). Large area hydrologic modeling and assessment Part I: Model development. *JAWRA Journal of the American Water Resources Association*, *34*(1), 73–89. https://doi.org/10.1111/j.1752-1688.1998.tb05961.x

Azzari, G., Grassini, P., Edreira, J. I. R., Conley, S., Mourtzinis, S., & Lobell, D. B. (2019). Satellite mapping of tillage practices in the North Central US region from 2005 to 2016. *Remote Sensing of Environment*, *221*, 417–429. https://doi.org/10.1016/j.rse.2018.11.010

Berhe, A. A., Harden, J. W., Torn, M. S., Kleber, M., Burton, S. D., & Harte, J. (2012). Persistence of soil organic matter in eroding versus depositional landform positions. *Journal of Geophysical Research*, *117*(G2). https://doi.org/10.1029/2011JG001790

Berhe, A. A., Harte, J., Harden, J. W., & Torn, M. S. (2007). The significance of the erosion-induced terrestrial carbon sink. *BioScience*, *57*(4), 337–346. https://doi.org/10.1641/B570408

Billings, S. A., Buddemeier, R. W., Richter, D. B., Van Oost, K., & Bohling, G. (2010). A simple method for estimating the influence of eroding soil profiles on atmospheric CO_2. *Global Biogeochemical Cycles*, *24*(2). https://doi.org/10.1029/2009GB003560

Billings, S. A., Richter, D. B., Ziegler, S. E., Prestegaard, K., & Wade, A. M. (2019). Distinct contributions of eroding and depositional profiles to land-atmosphere CO_2 exchange in two contrasting forests. *Frontiers in Earth Science*, *7*, 36. https://doi.org/10.3389/feart.2019.00036

Blair, N., Hayes, J. M., Grimley, D., & Anders, A. M. (2022). Eroded critical zone carbon and where to find it: Examples from the IML-CZO. In A. S. Wymore, W. H. Yang, W. L. Silver, W. H. McDowell, & J. Chorover (Eds.), *Biogeochemistry of the critical zone* (pp. 121–143). Springer International Publishing. https://doi.org/10.1007/978-3-030-95921-0_5

Borrelli, P., Robinson, D. A., Fleischer, L. R., Lugato, E., Ballabio, C., Alewell, C., et al. (2017). An assessment of the global impact of 21st century land use change on soil erosion. *Nature Communications*, *8*(1), 2013. https://doi.org/10.1038/s41467-017-02142-7

Borrelli, P., Robinson, D. A., Panagos, P., Lugato, E., Yang, J. E., Alewell, C., et al. (2020). Land use and climate change impacts on global soil erosion by water (2015–2070). *Proceedings of the National Academy of Sciences*, *117*(36), 21994–22001. https://doi.org/10.1073/pnas.2001403117

Christopher, S. F., Lal, R., & Mishra, U. (2009). Regional study of no-till effects on carbon sequestration in the Midwestern United States. *Soil Science Society of America Journal*, *73*(1), 207–216. https://doi.org/10.2136/sssaj2007.0336

Claassen, R., Bowman, M., McFadden, J., Smith, D., & Wallander, S. (2018). *Tillage intensity and conservation cropping in the United States* (No. EIB-197). U.S. Department of Agriculture, Economic Research Service. Retrieved from http://www.ers.usda.gov/publications/pub-details/?pubid=90200

Dalton, A. S., Margold, M., Stokes, C. R., Tarasov, L., Dyke, A. S., Adams, R. S., et al. (2020). An updated radiocarbon-based ice margin chronology for the last deglaciation of the North American Ice Sheet Complex. *Quaternary Science Reviews*, *234*, 106223. https://doi.org/10.1016/j.quascirev.2020.106223

De Jong-Hughes, J., & Daigh, A. L. M. (2017). *Tillage implements, purpose, and ideal use. In: Upper Midwest tillage guide. Part 2*. University of Minnesota Extension Service and North Dakota State University. https://extension.umn.edu/soil-management-and-health/tillage-implements

Doetterl, S., Berhe, A. A., Nadeu, E., Wang, Z., Sommer, M., & Fiener, P. (2016). Erosion, deposition and soil carbon: A review of process-level controls, experimental tools and models to address C cycling in dynamic landscapes. *Earth-Science Reviews*, *154*, 102–122. https://doi.org/10.1016/j.earscirev.2015.12.005

Doetterl, S., Van Oost, K., & Six, J. (2012). Towards constraining the magnitude of global agricultural sediment and soil organic carbon fluxes. *Earth Surface Processes and Landforms*, *37*(6), 642–655. https://doi.org/10.1002/esp.3198

Evans, D. L., Quinton, J. N., Tye, A. M., Rodés, Á., Davies, J. A. C., Mudd, S. M., & Quine, T. A. (2019). Arable soil formation and erosion: A hillslope-based cosmogenic nuclide study in the United Kingdom. *Soil*, *5*(2), 253–263. https://doi.org/10.5194/soil-5-253-2019

Fenton, T. E., Kazemi, M., & Lauterbach-Barrett, M. A. (2005). Erosional impact on organic matter content and productivity of selected Iowa soils. *Soil and Tillage Research*, *81*(2), 163–171. https://doi.org/10.1016/j.still.2004.09.005

Fernandes, N. F., & Dietrich, W. E. (1997). Hillslope evolution by diffusive processes: The timescale for equilibrium adjustments. *Water Resources Research*, *33*(6), 1307–1318. https://doi.org/10.1029/97WR00534

Food and Agriculture Organization of the United Nations. (2015). *Healthy soils are the basis for healthy food production*. FAO. Retrieved from http://www.fao.org/3/a-i4405e.pdf

Gelder, B., Sklenar, T., James, D., Herzmann, D., Cruse, R., Gesch, K., & Laflen, J. (2018). The Daily Erosion Project—Daily estimates of water runoff, soil detachment, and erosion: The Daily Erosion Project: Estimating Runoff and Soil Loss. *Earth Surface Processes and Landforms*, *43*(5), 1105–1117. https://doi.org/10.1002/esp.4286

Gelder, B. K., Anex, R. P., Kaspar, T. C., Sauer, T. J., & Karlen, D. L. (2011). Estimating soil organic carbon in Central Iowa using aerial imagery and soil surveys. *Soil Science Society of America Journal*, *75*(5), 1821–1828. https://doi.org/10.2136/sssaj2010.0260

Georgiou, K., Jackson, R. B., Vindušková, O., Abramoff, R. Z., Ahlström, A., Feng, W., et al. (2022). Global stocks and capacity of mineral-associated soil organic carbon. *Nature Communications*, *13*(1), 3797. https://doi.org/10.1038/s41467-022-31540-9

Govers, G., Vandaele, K., Desmet, P., Poesen, J., & Bunte, K. (1994). The role of tillage in soil redistribution on hillslopes. *European Journal of Soil Science*, *45*(4), 469–478. https://doi.org/10.1111/j.1365-2389.1994.tb00532.x

Gregorich, E. G., Greer, K. J., Anderson, D. W., & Liang, B. C. (1998). Carbon distribution and losses: Erosion and deposition effects. *Soil and Tillage Research*, *47*(3), 291–302. https://doi.org/10.1016/S0167-1987(98)00117-2

Harden, J. W., Sharpe, J. M., Parton, W. J., Ojima, D. S., Fries, T. L., Huntington, T. G., & Dabney, S. M. (1999). Dynamic replacement and loss of soil carbon on eroding cropland. *Global Biogeochemical Cycles*, *13*(4), 885–901. https://doi.org/10.1029/1999GB900061

Jennings, M. D. (2000). Gap analysis: Concepts, methods, and recent results. *Landscape Ecology*, *15*(1), 5–20. https://doi.org/10.1023/A:1008184408300

Kopittke, P. M., Menzies, N. W., Wang, P., McKenna, B. A., & Lombi, E. (2019). Soil and the intensification of agriculture for global food security. *Environment International*, *132*, 105078. https://doi.org/10.1016/j.envint.2019.105078

Kuhn, N. J., Hoffmann, T., Schwanghart, W., & Dotterweich, M. (2009). Agricultural soil erosion and global carbon cycle: Controversy over? *Earth Surface Processes and Landforms*, *34*(7), 1033–1038. https://doi.org/10.1002/esp.1796

Kumar, S., Kadono, A., Lal, R., & Dick, W. (2012). Long-term no-till impacts on organic carbon and properties of two contrasting soils and corn yields in Ohio. *Soil Science Society of America Journal*, *76*(5), 1798–1809. https://doi.org/10.2136/sssaj2012.0055

Kwang, J. S. (2022). jeffskwang/SOC_LEM_County_Simplified: SOC_LEM_County_Simplified (Version v1) [Computer software]. Zenodo. https://doi.org/10.5281/ZENODO.6647033

Kwang, J. S., Thaler, E., & Larsen, I. (2022). Forecasts of landscape evolution and soil organic carbon redistribution in the Midwestern United States [Dataset]. University of Massachusetts Amherst. https://doi.org/10.7275/TGMW-S318

Kwang, J. S., Thaler, E. A., Quirk, B. J., Quarrier, C. L., & Larsen, I. J. (2022). A landscape evolution modeling approach for predicting three-dimensional soil organic carbon redistribution in agricultural landscapes. *Journal of Geophysical Research: Biogeosciences*, *127*(2), e2021JG006616. https://doi.org/10.1029/2021JG006616

Laflen, J. M., Elliot, W. J., Simanton, J. R., Holzhey, C. S., & Kohl, K. D. (1991). WEPP: Soil erodibility experiments for rangeland and cropland soils. *Journal of Soil and Water Conservation*, *46*(1), 39–44.

Lal, R. (2003). Soil erosion and the global carbon budget. *Environment International*, *29*(4), 437–450. https://doi.org/10.1016/S0160-4120(02)00192-7

Lal, R. (2006). Enhancing crop yields in the developing countries through restoration of the soil organic carbon pool in agricultural lands. *Land Degradation & Development*, *17*(2), 197–209. https://doi.org/10.1002/ldr.696

Lal, R. (2019). Accelerated Soil erosion as a source of atmospheric CO_2. *Soil and Tillage Research*, *188*, 35–40. https://doi.org/10.1016/j.still.2018.02.001

Lal, R., & Pimentel, D. (2008). Soil erosion: A carbon sink or source? *Science*, *319*(5866), 1040–1042. https://doi.org/10.1126/science.319.5866.1040

Lal, R., Reicosky, D. C., & Hanson, J. D. (2007). Evolution of the plow over 10,000 years and the rationale for no-till farming. *Soil and Tillage Research*, *93*(1), 1–12. https://doi.org/10.1016/j.still.2006.11.004

Li, X., McCarty, G. W., Karlen, D. L., & Cambardella, C. A. (2018). Topographic metric predictions of soil redistribution and organic carbon in Iowa cropland fields. *Catena*, *160*, 222–232. https://doi.org/10.1016/j.catena.2017.09.026

Lindstrom, M. J., Nelson, W. W., Schumacher, T. E., & Lemme, G. D. (1990). Soil movement by tillage as affected by slope. *Soil and Tillage Research*, *17*(3), 255–264. https://doi.org/10.1016/0167-1987(90)90040-K

Liu, S., Bliss, N., Sundquist, E., & Huntington, T. G. (2003). Modeling carbon dynamics in vegetation and soil under the impact of soil erosion and deposition. *Global Biogeochemical Cycles*, *17*(2). https://doi.org/10.1029/2002GB002010

Lobb, D. A., Kachanoski, R. G., & Miller, M. H. (1995). Tillage translocation and tillage erosion on shoulder slope landscape positions measured using 137Cs as a tracer. *Canadian Journal of Soil Science*, *75*(2), 211–218. https://doi.org/10.4141/cjss95-029

Lobb, D. A., Kachanoski, R. G., & Miller, M. H. (1999). Tillage translocation and tillage erosion in the complex upland landscapes of southwestern Ontario, Canada. *Soil and Tillage Research*, *51*(3), 189–209. https://doi.org/10.1016/S0167-1987(99)00037-9

Loisel, J., Casellas Connors, J. P., Hugelius, G., Harden, J. W., & Morgan, C. L. (2019). Soils can help mitigate CO_2 emissions, despite the challenges. *Proceedings of the National Academy of Sciences*, *116*(21), 10211–10212. https://doi.org/10.1073/pnas.1900444116

Luo, Z., Wang, E., & Sun, O. J. (2010). Can no-tillage stimulate carbon sequestration in agricultural soils? A meta-analysis of paired experiments. *Agriculture, Ecosystems & Environment*, *139*(1), 224–231. https://doi.org/10.1016/j.agee.2010.08.006

Manies, K. L., Harden, J. W., Kramer, L., & Parton, W. J. (2001). Carbon dynamics within agricultural and native sites in the loess region of western Iowa. *Global Change Biology*, *7*(5), 545–555. https://doi.org/10.1046/j.1354-1013.2001.00427.x

Meersmans, J., Van Wesemael, B., De Ridder, F., Fallas Dotti, M., De Baets, S., & Van Molle, M. (2009). Changes in organic carbon distribution with depth in agricultural soils in northern Belgium, 1960–2006. *Global Change Biology*, *15*(11), 2739–2750. https://doi.org/10.1111/j.1365-2486.2009.01855.x

Mikhailova, E. A., Altememe, A. H., Bawazir, A. A., Chandler, R. D., Cope, M. P., Post, C. J., et al. (2016). Comparing soil carbon estimates in glaciated soils at a farm scale using geospatial analysis of field and SSURGO data. *Geoderma*, *281*, 119–126. https://doi.org/10.1016/j.geoderma.2016.06.029

Mollinedo, J. (2008). *Tillage erosion coefficients for selected tillage tools*. (M.S.). South Dakota State University. Retrieved from https://www.proquest.com/docview/304464603/abstract/8048E54E235E4AC3PQ/1

Montgomery, D. R. (2007a). *Dirt: The erosion of civilizations* (1st ed.). University of California Press.

Montgomery, D. R. (2007b). Soil erosion and agricultural sustainability. *Proceedings of the National Academy of Sciences*, *104*(33), 13268–13272. https://doi.org/10.1073/pnas.0611508104

Montgomery, D. R. (2017). *Growing a revolution: Bringing our soil back to life*. W. W. Norton & Company.

Montgomery, D. R., Biklé, A., Archuleta, R., Brown, P., & Jordan, J. (2022). Soil health and nutrient density: Preliminary comparison of regenerative and conventional farming. *PeerJ*, *10*, e12848. https://doi.org/10.7717/peerj.12848

Nadeu, E., Berhe, A. A., de Vente, J., & Boix-Fayos, C. (2012). Erosion, deposition and replacement of soil organic carbon in Mediterranean catchments: A geomorphological, isotopic and land use change approach. *Biogeosciences*, *9*(3), 1099–1111. https://doi.org/10.5194/bg-9-1099-2012

Nadeu, E., Gobin, A., Fiener, P., van Wesemael, B., & van Oost, K. (2015). Modelling the impact of agricultural management on soil carbon stocks at the regional scale: The role of lateral fluxes. *Global Change Biology*, *21*(8), 3181–3192. https://doi.org/10.1111/gcb.12889

National Science and Technology Council. (2016). The state and future of U.S. soils. Retrieved from https://obamawhitehouse.archives.gov/sites/default/files/microsites/ostp/ssiwg_framework_december_2016.pdf

Natural Resources Conservation Service. (2021). Mollisols map. Retrieved from https://www.nrcs.usda.gov/wps/portal/nrcs/detail/soils/survey/class/maps/?cid=nrcs142p2_053604

Nunes, M. R., Karlen, D. L., Veum, K. S., Moorman, T. B., & Cambardella, C. A. (2020). Biological soil health indicators respond to tillage intensity: A US meta-analysis. *Geoderma*, *369*, 114335. https://doi.org/10.1016/j.geoderma.2020.114335

Olmstead, A. L., & Rhode, P. W. (2001). Reshaping the landscape: The impact and diffusion of the tractor in American agriculture, 1910–1960. *The Journal of Economic History*, *61*(3), 663–698. https://doi.org/10.1017/S0022050701030042

O'Neal, M. R., Nearing, M. A., Vining, R. C., Southworth, J., & Pfeifer, R. A. (2005). Climate change impacts on soil erosion in Midwest United States with changes in crop management. *Catena*, *61*(2), 165–184. https://doi.org/10.1016/j.catena.2005.03.003

Papiernik, S. K., Schumacher, T. E., Lobb, D. A., Lindstrom, M. J., Lieser, M. L., Eynard, A., & Schumacher, J. A. (2009). Soil properties and productivity as affected by topsoil movement within an eroded landform. *Soil and Tillage Research*, *102*(1), 67–77. https://doi.org/10.1016/j.still.2008.07.018

Pennock, D. J., & De Jong, E. (1987). The influence of slope curvature on soil erosion and deposition in hummock terrain. *Soil Science*, *144*(3), 209–217. https://doi.org/10.1097/00010694-198709000-00007

Petr, N., & Josef, H. (2018). Translocation of soil particles during secondary soil tillage along contour lines. *Water*, *10*(5), 568. https://doi.org/10.3390/w10050568

Pimentel, D., Harvey, C., Resosudarmo, P., Sinclair, K., Kurz, D., McNair, M., et al. (1995). Environmental and economic costs of soil erosion and conservation benefits. *Science*, *267*(5201), 1117–1123. https://doi.org/10.1126/science.267.5201.1117

Powlson, D. S., Stirling, C. M., Jat, M. L., Gerard, B. G., Palm, C. A., Sanchez, P. A., & Cassman, K. G. (2014). Limited potential of no-till agriculture for climate change mitigation. *Nature Climate Change*, *4*(8), 678–683. https://doi.org/10.1038/nclimate2292

Quarrier, C. L., Kwang, J. S., Quirk, B. J., Thaler, E. A., & Larsen, I. J. (2022). Pre-agricultural soil erosion rates in the Midwestern United States. *Geology*, *51*(1), 44–48. https://doi.org/10.1130/G50667.1

Quine, T. A., & Oost, K. V. (2007). Quantifying carbon sequestration as a result of soil erosion and deposition: Retrospective assessment using caesium-137 and carbon inventories. *Global Change Biology*, *13*(12), 2610–2625. https://doi.org/10.1111/j.1365-2486.2007.01457.x

Quinton, J. N., Govers, G., Van Oost, K., & Bardgett, R. D. (2010). The impact of agricultural soil erosion on biogeochemical cycling. *Nature Geoscience*, *3*(5), 311–314. https://doi.org/10.1038/ngeo838

Renard, K. G., Foster, G. R., Weesies, G. A., McCool, D. K., & Yoder, D. C. (1997). Predicting soil erosion by water: a guide to conservation planning with the revised universal soil loss equation (RUSLE). USDA-ARS, Agriculture handbook No. 703.

Reusser, L., Bierman, P., & Rood, D. (2015). Quantifying human impacts on rates of erosion and sediment transport at a landscape scale. *Geology*, *43*(2), 171–174. https://doi.org/10.1130/G36272.1

Rosenbloom, N. A., Doney, S. C., & Schimel, D. S. (2001). Geomorphic evolution of soil texture and organic matter in eroding landscapes. *Global Biogeochemical Cycles*, *15*(2), 365–381. https://doi.org/10.1029/1999GB001251

Rosenbloom, N. A., Harden, J. W., Neff, J. C., & Schimel, D. S. (2006). Geomorphic control of landscape carbon accumulation. *Journal of Geophysical Research*, *111*(G1), G01004. https://doi.org/10.1029/2005JG000077

Samson, F., & Knopf, F. (1994). Prairie conservation in North America. *BioScience*, *44*(6), 418–421. https://doi.org/10.2307/1312365

Sanderman, J., Hengl, T., & Fiske, G. J. (2017). Soil carbon debt of 12,000 years of human land use. *Proceedings of the National Academy of Sciences*, *114*(36), 9575–9580. https://doi.org/10.1073/pnas.1706103114

Schneider, S. K., Cavers, C. G., Duke, S. E., Schumacher, J. A., Schumacher, T. E., & Lobb, D. A. (2021). Crop responses to topsoil replacement within eroded landscapes. *Agronomy Journal*, *113*(3), 2938–2949. https://doi.org/10.1002/agj2.20635

Shukla, P. R., Skea, J., Calvo Buendia, E., Masson-Delmotte, V., Pörtner, H.-O., Roberts, D. C., et al. (2019). *IPCC, 2019: Climate Change and Land: An IPCC special report on climate change, desertification, land degradation, sustainable land management, food security, and greenhouse gas fluxes in terrestrial ecosystems*. (Report). Intergovernmental Panel on Climate Change (IPCC). https://doi.org/10.25561/76618

Smith, S. V., Renwick, W. H., Buddemeier, R. W., & Crossland, C. J. (2001). Budgets of soil erosion and deposition for sediments and sedimentary organic carbon across the conterminous United States. *Global Biogeochemical Cycles*, *15*(3), 697–707. https://doi.org/10.1029/2000GB001341

Soil Survey Staff. (2013). *Rapid Carbon Assessment (RaCA) project*. United States Department of Agriculture, Natural Resources Conservation Service. Retrieved from https://data.nal.usda.gov/dataset/rapid-carbon-assessment-raca

Soil Survey Staff. (2020). *Gridded Soil Survey Geographic (gSSURGO) database for the United States of America and the territories, Commonwealths, and Island Nations served by the USDA-NRCS*. United States Department of Agriculture, Natural Resources Conservation Service. Retrieved from https://gdg.sc.egov.usda.gov/

Stallard, R. F. (1998). Terrestrial sedimentation and the carbon cycle: Coupling weathering and erosion to carbon burial. *Global Biogeochemical Cycles*, *12*(2), 231–257. https://doi.org/10.1029/98GB00741

Sulman, B. N., Harden, J., He, Y., Treat, C., Koven, C., Mishra, U., et al. (2020). Land use and land cover affect the depth distribution of soil carbon: Insights from a large database of soil profiles. *Frontiers in Environmental Science*, *8*, 146. https://doi.org/10.3389/fenvs.2020.00146

Thaler, E. A., Kwang, J. S., Quirk, B. J., Quarrier, C. L., & Larsen, I. J. (2022). Rates of historical anthropogenic soil erosion in the Midwestern United States. *Earth's Future*, *10*(3), e2021EF002396. https://doi.org/10.1029/2021EF002396

Thaler, E. A., Larsen, I. J., & Yu, Q. (2021). The extent of soil loss across the US Corn Belt. *Proceedings of the National Academy of Sciences*, *118*(8), e1922375118. https://doi.org/10.1073/pnas.1922375118

Tilman, D., Cassman, K. G., Matson, P. A., Naylor, R., & Polasky, S. (2002). Agricultural sustainability and intensive production practices. *Nature*, *418*(6898), 671–677. https://doi.org/10.1038/nature01014

Tomer, M. D., James, D. E., & Sandoval-Green, C. M. J. (2017). Agricultural conservation planning framework: 3. Land use and field boundary database development and structure. *Journal of Environmental Quality*, *46*(3), 676–686. https://doi.org/10.2134/jeq2016.09.0363

U.S. Department of Agriculture. (2018). *Summary report; 2017 national resources inventory*. Natural Resources Conservation Service and Center for Survey Statistics and Methodology, Iowa State University. Retrieved from https://www.nrcs.usda.gov/wps/portal/nrcs/main/national/technical/nra/nri/results/

U.S. Department of Agriculture. (2020). Crop production 2020 summary 01/12/2021. Crop Production, 125.

US EPA, O. (2015). Level III and IV ecoregions of the continental United States. [Data and tools]. Retrieved August 31, 2021, from Retrieved from https://www.epa.gov/eco-research/level-iii-and-iv-ecoregions-continental-united-states

U.S. Geological Survey. (2020). National transportation dataset. Retrieved from https://nationalmap.gov/transport.html

U.S. Geological Survey. (2021). National hydrography dataset. Retrieved from https://www.usgs.gov/national-hydrography/access-national-hydrography-products

VandenBygaart, A. J. (2001). Erosion and deposition history derived by depth-stratigraphy of 137Cs and soil organic carbon. *Soil and Tillage Research*, *61*(3), 187–192. https://doi.org/10.1016/S0167-1987(01)00203-3

Van Muysen, W., Van Oost, K., & Govers, G. (2006). Soil translocation resulting from multiple passes of tillage under normal field operating conditions. *Soil and Tillage Research*, *87*(2), 218–230. https://doi.org/10.1016/j.still.2005.04.011

Van Oost, K., Govers, G., De Alba, S., & Quine, T. A. (2006). Tillage erosion: A review of controlling factors and implications for soil quality. *Progress in Physical Geography: Earth and Environment*, *30*(4), 443–466. https://doi.org/10.1191/0309133306pp487ra

Van Oost, K., Govers, G., & Desmet, P. (2000). Evaluating the effects of changes in landscape structure on soil erosion by water and tillage. *Landscape Ecology*, *15*(6), 577–589. https://doi.org/10.1023/A:1008198215674

Van Oost, K., Govers, G., Quine, T. A., Heckrath, G., Olesen, J. E., De Gryze, S., & Merckx, R. (2005). Landscape-scale modeling of carbon cycling under the impact of soil redistribution: The role of tillage erosion. *Global Biogeochemical Cycles*, *19*(4). https://doi.org/10.1029/2005GB002471

Van Oost, K., Quine, T. A., Govers, G., De Gryze, S., Six, J., Harden, J. W., et al. (2007). The impact of agricultural soil erosion on the global carbon cycle. *Science*, *318*(5850), 626–629. https://doi.org/10.1126/science.1145724

Van Oost, K., & Six, J. (2023). Reconciling the paradox of soil organic carbon erosion by water. *Biogeosciences*, *20*(3), 635–646. https://doi.org/10.5194/bg-20-635-2023

West, T. O., Marland, G., King, A. W., Post, W. M., Jain, A. K., & Andrasko, K. (2004). Carbon management response curves: Estimates of temporal soil carbon dynamics. *Environmental Management*, *33*(4), 507–518. https://doi.org/10.1007/s00267-003-9108-3

West, T. O., & Post, W. M. (2002). Soil organic carbon sequestration rates by tillage and crop rotation. *Soil Science Society of America Journal*, *66*(6), 1930–1946. https://doi.org/10.2136/sssaj2002.1930

Weyer, P. J., Cerhan, J. R., Kross, B. C., Hallberg, G. R., Kantamneni, J., Breuer, G., et al. (2001). Municipal drinking water nitrate level and cancer risk in older women: The Iowa Women's health Study. *Epidemiology*, *12*(3), 327–338. https://doi.org/10.1097/00001648-200105000-00013

Wills, S., Loecke, T., Sequeira, C., Teachman, G., Grunwald, S., & West, L. T. (2014). Overview of the U.S. Rapid carbon assessment project: Sampling design, initial summary and uncertainty estimates. In A. E. Hartemink & K. McSweeney (Eds.), *Soil carbon* (pp. 95–104). Springer International Publishing. https://doi.org/10.1007/978-3-319-04084-4_10

Wischmeier, W. H., & Smith, D. D. (1978). Predicting rainfall erosion losses: A guide to conservation planning. (Agricultural Handbook No. 537) (p. 58).

Yan, Q., Le, P. V. V., Woo, D. K., Hou, T., Filley, T., & Kumar, P. (2019). Three-dimensional modeling of the coevolution of landscape and soil organic carbon. *Water Resources Research*, *55*(2), 1218–1241. https://doi.org/10.1029/2018WR023634

Young, C. J., Liu, S., Schumacher, J. A., Schumacher, T. E., Kaspar, T. C., McCarty, G. W., et al. (2014). Evaluation of a model framework to estimate soil and soil organic carbon redistribution by water and tillage using 137Cs in two U.S. Midwest agricultural fields. *Geoderma*, *232–234*, 437–448. https://doi.org/10.1016/j.geoderma.2014.05.019

Zhong, B., & Xu, Y. J. (2011). Scale effects of geographical soil datasets on soil carbon estimation in Louisiana, USA: A comparison of STATSGO and SSURGO. *Pedosphere*, *21*(4), 491–501. https://doi.org/10.1016/S1002-0160(11)60151-3